

MASTER THESIS

WHITE BLOOD CELL DEPLETION OF IMMUNOMAGNETICALLY ENRICHED SAMPLES USING ANTIBODY FUNCTIONALISED SURFACES

UNIVERSITY OF TWENTE | MEDICAL CELL BIOPHYSICS

BIOMEDICAL ENGINEERING | BIOENGINEERING TECHNOLOGIES

AUTHOR

F.G.A. DUIJKERS

SUPERVISOR(S)

IR. M. STEVENS

PROF. DR. L.W.M.M. TERSTAPPEN

PROF. DR. IR. P. JONKHEIJM

DR. R. BANSAL

24/08/2023



UNIVERSITY OF TWENTE.

ACKNOWLEDGEMENTS

I would like to thank Ruchi Bansal and Leon Terstappen and for giving me the opportunity to carry out my master thesis at Medical Cell BioPhysics (MCBP). In addition, I would like to express my gratitude to my daily supervisor, Michiel Stevens, who guided me throughout this project. He was always able to meet and discuss all my questions. I would like to thank everyone that attended the Cancer Watch meetings for their expert advice and critical view throughout this project. I wish to acknowledge the help provided by the technical staff Christian Breukers, Anouk Mentink and Yvonne Kraan, and the other members of the MCBP group, for their help with the experiments. Special thanks to my friends, family and boyfriend for their support during my master thesis. Lastly, I would like to thank Ruchi Bansal, Pascal Jonkheijm, Leon Terstappen, and Michiel Stevens for their willingness to be part of the exam committee and all their help throughout the project.

TABLE OF CONTENT

| | |
|--|-----------|
| LIST OF ABBREVIATIONS | 4 |
| SUMMARY | 5 |
| 1 INTRODUCTION | 6 |
| 2 THEORETICAL BACKGROUND | 7 |
| 2.1 PROBLEM DESCRIPTION AND RESEARCH QUESTION..... | 7 |
| 2.2 ASSESSMENT OF THE TECHNIQUE | 9 |
| 2.3 ANTIBODY FUNCTIONALISATION OF GLASS- AND HYDROGEL SURFACES | 10 |
| 2.4 CELL CAPTURE | 10 |
| 3 METHODS | 12 |
| 3.1 SAMPLE PREPARATION | 12 |
| 3.2 EXPERIMENTAL SETUP | 13 |
| 3.3 SURFACE MODIFICATION..... | 13 |
| 3.4 CELL CAPTURE ON THE COATED SURFACE | 15 |
| 3.5 IMAGE ACQUISITION AND ANALYSIS | 15 |
| 3.6 TUMOR CELL RECOVERY OF THE DEPLETED SAMPLE | 16 |
| 4 RESULTS | 17 |
| 4.1 ESTABLISHMENT OF A WHITE BLOOD CELL DEPLETION TECHNIQUE | 17 |
| 4.2 EFFICIENCY OF WHITE BLOOD CELL DEPLETION ON A MULTIWELL SLIDE..... | 24 |
| 4.3 TUMOR CELL COLLECTION AFTER WHITE BLOOD CELL DEPLETION | 29 |
| 5 DISCUSSION | 32 |
| 5.1 DISCUSSION..... | 32 |
| 5.2 RECOMMENDATIONS FOR FURTHER RESEARCH..... | 35 |
| 5.3 CONCLUSION | 37 |
| 6 REFERENCES | 38 |
| 7 APPENDICES | 42 |
| 7.1 ANTIBODY CONCENTRATION ON HYDROGEL..... | 42 |
| 7.2 CELL CAPTURE AND WASHING SPEED AND -TIME | 43 |
| 7.3 FLOW CHANNEL BEFORE- AND AFTER WASHING..... | 44 |
| 7.4 FLOW CYTOMETRY SCATTERPLOTS OF STAINED AND UNSTAINED CELLS | 44 |
| 7.5 CALCULATIONS BASED ON FLOW CYTOMETRY OF WBC DEPLETED SAMPLE INCLUDING THE THIRD POPULATION | 45 |
| 7.6 RED BLOOD CELLS ON THE COATED SURFACE | 46 |

LIST OF ABBREVIATIONS

| <i>Abbreviation</i> | <i>Explanation</i> |
|---------------------|--|
| <i>APTES</i> | (3-aminopropyl)triethoxysilane |
| <i>BSA</i> | Bovine serum albumin |
| <i>CD15</i> | 3-fucosyl-N-acetyl-lactosamine |
| <i>CD16</i> | Fc-gamma receptor III |
| <i>CD45</i> | Leukocyte common antigen |
| <i>CS&T</i> | Cytometer Setup and Tracking |
| <i>CTC</i> | Circulating Tumor Cell |
| <i>CTO</i> | CellTracker Orange |
| <i>DAPI</i> | 4',6-diamidino-2-phenylindole |
| <i>DFF</i> | Dean Flow Fractionation |
| <i>DLA</i> | Diagnostic Leukapheresis |
| <i>ECTM</i> | Experimental Centre for Technical Medicine |
| <i>EDC/NHS</i> | 1-Ethyl-3-[3-dimethylami- nopropyl]-carbodiimide hydrochloride |
| <i>EpCAM</i> | epithelial cell adhesion activating molecule |
| <i>FACS</i> | Fluorescence Activated Cell Sorting |
| <i>FBS</i> | Fetal Bovine Serum |
| <i>FDA</i> | Food and Drug Administration |
| <i>FSC-A</i> | Forward Scatter Area |
| <i>HI30</i> | CD45 Monoclonal Antibody |
| <i>HNaPO4</i> | Disodium phosphate |
| <i>Hoechst</i> | 2'-(4-Ethoxyphenyl)-5-(4-methyl-1-piperazinyl)-2,5'-bi-1H-benzimidazole trihydrochloride |
| <i>IgG-PE</i> | PE-conjugated IgG polymer |
| <i>LCL</i> | Lymphoblastoid Cell Line |
| <i>LNCaP</i> | Lymph Node Carcinoma of the Prostate |
| <i>MgSO4</i> | Magnesium sulfate |
| <i>MNC</i> | Mononuclear Cell |
| <i>PBS</i> | Phosphate-buffered saline |
| <i>PC3</i> | Human prostate cancer cell |
| <i>PCR</i> | Polymerase chain reaction |
| <i>PE</i> | Phycoerythrin |
| <i>PEG</i> | Polyethylene glycol |
| <i>Pen/Strep</i> | Penicillin-streptomycin |
| <i>RBC</i> | Red Blood Cell |
| <i>ROI</i> | Region of Interest |
| <i>RosetteSEP</i> | Human T Cell Enrichment Cocktail that is designed to isolate T cells from whole blood by negative selection. |
| <i>SPR</i> | Surface Plasmon Resonance |
| <i>SSC-A</i> | Side Scatter Area |
| <i>VU1D9</i> | Mouse mAb that targets EpCAM |
| <i>WBC</i> | White Blood Count |

SUMMARY

Significance Cancer is a leading cause of death worldwide. In patients with cancer, CTCs can give insight into tumor status and treatment effectiveness. These rare cells can be enriched from blood samples using CellSearch, which uses immunomagnetic particles that target CTCs and magnetism to capture them. DLA can overcome the low-frequency problem of CTCs by enabling the screening of high blood volumes. Currently, a high overflow of non-specifically captured WBCs in immunomagnetically enriched samples limits the efficient characterisation of CTCs and the ability to process DLA samples.

Aim This research aimed to develop a technique to deplete WBCs from immunomagnetically enriched samples using an antibody-coated surface. This way, the number of non-specifically captured WBCs in the sample can be reduced.

Approach First, antibodies specifically targeted at WBCs were immobilised on a surface. Then, (immunomagnetically enriched) samples containing WBCs and TCs were centrifuged on top of it and thereby promoted to bind to that surface. Through washing off the unbound cells and collecting the remaining sample, WBCs were depleted. Two types of surfaces were coated with anti-CD45 antibodies; a glass- and hydrogel surface, using respective protocols.

Results The data presented in this research demonstrates that one-third of WBCs can be depleted from immunomagnetically enriched samples on an antibody-coated surface while 96% of tumor cells are washed off. As expected, the cell capture of immunomagnetically enriched samples was significantly reduced compared to non-immunomagnetically enriched samples. The cell capture on both tested surface types was fairly similar for WBC binding, while less non-specific binding of PC3 cells was measured on the glass surface. This is substantiated by the higher enrichment factor of a non-enriched sample on glass (11x) compared to hydrogel (5x). However, the recovery of cells in the collected sample was not measured but merely the enrichment factor determined from a part of the sample. Further research and optimisation are recommended to get a better picture of cell recovery and factors affecting the technique's performance, such as the flow speed used for washing.

Conclusions In conclusion, this research presents a technique for the depletion of WBCs from immunomagnetically enriched samples using an antibody-coated glass- and hydrogel surface. Out of the two tested surface types, the coated glass surface performed best because less non-specific binding of TCs was observed. Further testing is needed to assess the cell recovery in the depleted sample. Nonetheless, the presented technique shows potential to enable the screening of large blood volumes of cancer patients through WBC depletion of immunomagnetically enriched samples.

1

INTRODUCTION

Every year, 120.000 people in the Netherlands are diagnosed with cancer, while 45.000 die from the disease [1]. To reduce this mortality, it is essential to quickly find the best treatment, which can only be achieved by regular evaluation of the treatment's effectiveness. Ideally, this evaluation also allows for the detection of acquired resistance or new tumor mutations.

A way to achieve such an insight into the tumor status and the effectiveness of the treatment is the isolation and characterisation of circulating tumor cells (CTCs) [2]. These tumor cells have entered the bloodstream and are the main cause of metastasis. By isolating CTCs and identifying their characteristics, the changes in the tumor can be identified on a regular basis. Evaluation of CTCs at any time during the course of the disease allows assessment of patient prognosis and is predictive of overall survival [3–5]. Besides enabling personalised medicine, CTC characterisation can be used to identify new therapeutic targets, elucidate drug resistance mechanisms, and improve our understanding of tumor progression and metastatic disease [6,7].

To assess the tumor status based on isolated CTCs in a patient, a sufficient amount of CTCs needs to be identified. CTCs are very rare; in a standard 7.5 mL blood sample, on average, only a few are found [8]. In 20-40% of metastatic cancer patients, no CTCs are found using the standard test. A dramatic increase in sample volume is needed to overcome the low-frequency problem of CTCs and screen higher blood volumes [3]. This can be achieved by means of diagnostic leukapheresis (DLA) [9,10].

In this procedure, mononuclear cells (MNCs) with a density of 1.055–1.08 g/mL are collected from peripheral blood via continuous centrifugation while the remaining components are returned to the patient. Since epithelial cells have similar density compared to MNCs, the portion of the blood that is extracted includes the CTCs. The resulting product contains many more CTCs, but also many more healthy cells than a standard 7.5 mL blood sample [11]. This way, the sampling volume can be increased from 7.5 mL to 7.5 L with little burden for the patient [12].

The currently only FDA-approved method for extraction of the rare CTCs from the blood and leukapheresis material is CellSearch [7]. This technique is based on immunomagnetic enrichment, in which magnetic nanoparticles are coated with an antibody directed against a specific marker that is present on tumor cells. By magnetically separating the magnetic particles, the tumor cells can be separated from the healthy blood cells [8]. Due to the high number of white blood cells in the leukapheresis material, the number of healthy cells captured by these particles prevents efficient identification and isolation of single CTCs [11,13,14]. A technique to deplete the white blood cells from immunomagnetically enriched samples could solve this problem. In this report, the development of a WBC depletion technique which is targeted at depleting immunomagnetically enriched samples is described.

In this report, the relevant theoretical background information is given in Chapter 2. Then the methods used for this research are described in Chapter 3. Next, the results are presented in Chapter 4. The results are discussed in Chapter 5, including recommendations for further research and a summary of the conclusions of this thesis.

2

THEORETICAL BACKGROUND

2.1 PROBLEM DESCRIPTION AND RESEARCH QUESTION

To give a clear picture of the problem being addressed in this study, this chapter first explains why an improvement in current techniques is needed. Then, existing alternatives are briefly discussed. Finally, the proposed solution is introduced along with the main research question.

2.1.1 Number of CTCs Required for Characterisation

CTCs from metastatic cancer patients can originate from a variety of metastatic sites. To characterise this tumour heterogeneity and monitor changes, analysis of CTCs at the single-cell level is needed. Gaining insight into the tumor dynamics associated with these different sites requires genomic, transcriptomic, proteomic and functional analysis [2]. Techniques to perform this characterisation of single CTCs and their isolation exist, such as FACS [15], DEPArray[16,17], Punch [18–20] or micromanipulation [21]. However, the use of these methods is associated with cell loss [10]. In addition, captured CTCs are frequently in poor condition, making the molecular analysis of the usually few CTCs challenging [22]. Taken together, their heterogeneity, poor condition and low abundance result in a high number of CTC needed to characterise the tumor status. Therefore, the more tumor cells are available, the better the chance to accurately characterise them [10].

2.1.2 Processing DLA Samples

Although DLA allows us to obtain vast numbers of CTCs, processing the DLA material provides new challenges due to the excess of WBCs in the sample [11,12,23]. In previous research, the average volume of DLA products was 53 mL (range 21-98, SD 16 mL), and the mononuclear blood fraction represented ~ 1.6 L of blood (range 0.03-3.5 L, SD 0.7 L) [10]. Due to the high MNC concentration resulting in high leukocyte-carry-over hindering CTC detection, only around 5% (200 million cells) of the total DLA product can be directly processed in a single CellSearch run without overloading the system [10,24]. This means that most of the DLA product, and therefore the majority of CTCs, cannot be processed in a single CellSearch run. Moreover, processing 200 million cells with CellSearch can already result in a carryover that is too high for accurate identification of CTC [10,24]. A simple solution to this problem is to dilute the sample and divide it over multiple cartridges for scanning and image analysis. However, this in turn creates other problems, such as that it involves a large amount of resources, time and thus cost [10]. To process DLA towards a product that can be used for downstream analysis, two important challenges must be faced: the ability to process large amounts of sample and the ability to reduce the number of leukocytes in a DLA sample from several billion to several thousands of cells. This means that further improvements of CTC enrichment technologies are needed to truly gain advantages of DLA as a means to obtain sufficient CTCs for the characterisation of the tumor and ultimately to guide therapy.

2.1.3 White Blood Cell Depletion

A way to tackle the high leukocyte-carry-over problem of processing DLA in the CellSearch system is by depletion of the MNC from the DLA product. For example, a technique that is currently used in clinical research to process DLA product before immunomagnetic enrichment of the target cells is RosetteSep. Here, the unwanted cells are crosslinked to red blood cells (RBC) by specific antibodies forming dense immunorosettes. The immunorosettes pellet during density gradient centrifugation. This leaves the untouched, purified target cells at the interface between the plasma and the density gradient medium [25]. However, there are multiple downsides to this technique. Most importantly, the WBC depletion is not effective enough. The residual WBCs that remain in the sample after WBC depletion hinder the identification and enumeration of CTCs in a sample [11,23]. In addition, CTCs could be lost during centrifugation either due to non-specific binding to the used antibodies or entrapment in the cell formations [24]. Next to that, to perform the RosetteSep protocol for the whole DLA product, a substantial amount of material is needed: enough RBCs of the patient to form immunorosettes, RosetteSep crosslinking antibodies, tubes and density gradient medium. Other technologies to deplete the unwanted cells

include the EasySep® system [26], the Quadrupole Magnetic Separator (QMS) [27], MACS [28] and CTC-iChip [29]. These techniques use antibodies targeting leukocyte-associated antigens that are tethered to magnetic particles. As CellSearch is also based on immunomagnetic cell capture, combining these techniques is insufficient to deplete unwanted cells [14]. Therefore, techniques that are not based on immunomagnetic separation should be considered.

2.1.4 Non-Immunomagnetic Cell Capture Techniques

While CellSearch is the only FDA-approved method, various alternative techniques for CTC enrichment have been reported in literature that do not rely on immunomagnetic separation [6,7]. These techniques target the biological or physical properties of CTCs. They can be categorised as size-based, immunoaffinity-based, and density-based methods or combinations of these methods to perform positive as well as negative enrichment for separation (Figure 1) [7]. Physical properties of CTCs include cell size[30,31], deformability, and electrical properties [32,33]. Biophysical enrichment techniques are label-free, fast and typically easier to operate, yet they lack specificity, particularly when discriminating CTCs from nucleated blood cells. [7,32,33]. The purity of CTCs in the final sample is greatly affected by the specificity of the method used. In affinity-based techniques, a high specificity can be achieved, as this is determined by the specificity of the chosen antibodies. Recently, microfluidics-based platforms have been widely integrated into numerous research areas. Previous studies show high CTC capture rates using a microfluidic device coated with antibodies to capture the CTCs [34–37]. They have been reported to efficiently capture cells with as few as 2,000 antigen molecules per cell [35]. It is however difficult to pinpoint a superior technique as the techniques have been tested in different ways: different cancer types, samples and testing and analysis methods. Moreover, some have been tested exclusively on cell lines and others have also successfully identified and isolated CTCs from clinical samples. We can however learn from the technical hurdles mentioned by these studies, which are the need for a large surface, low sample throughput, reliability and long processing times.

The technique tested in this research project is a combined technique that uses negative enrichment, immunocapture and fluidics to separate WBC and TCs, as indicated in Figure 1.

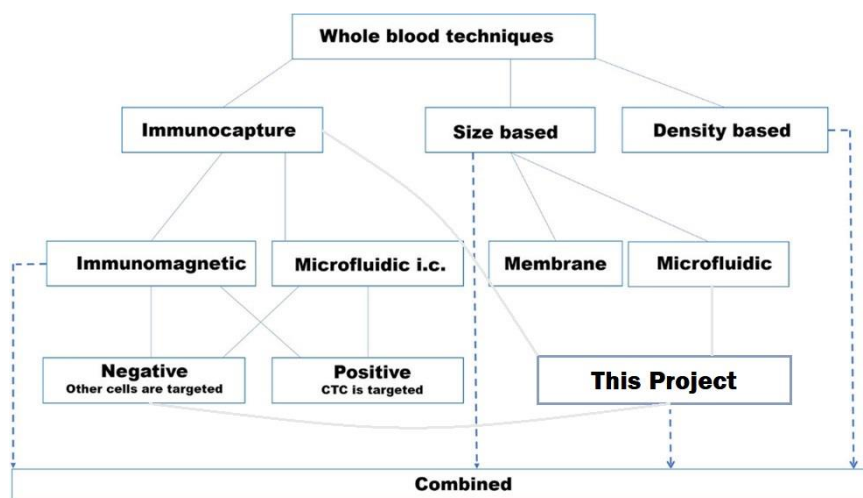


Figure 1 Different types of whole blood methods where immunocapture and physical selection (size and density) methods are separated into subgroups depending on the main properties of the technique. ("Immunoaffinity," "Size based," "Density based" and "Combined") Adapted from [7]

2.1.5 White Blood Cell Depletion of Immunomagnetically Enriched Samples

One way to improve the purity of CTCs for characterisation and to increase the amount of sample that can be processed might be to perform immunomagnetic enrichment of CTCs before depletion of background cells. That way, most MNCs will already have been removed from the sample during immunomagnetic enrichment. The remaining sample includes the immunomagnetically captured CTCs and MNCs that have been captured due to e.g. non-specific binding of the immunomagnetic nanoparticles. To give an indication, CellSearch enrichment has been reported to reach over 99.9% (4 log) depletion of leukocytes when processing 7.5mL whole blood samples. However, it can still leave around 800 contaminating WBCs in the immunomagnetically enriched sample [14]. The WBC contamination is higher in DLA samples [11,12]. The following step is to deplete these MNCs. It is

hypothesised that because all cells in the samples are immunomagnetically labelled, applying standard white blood cell depletion protocols will be less efficient. Therefore, other techniques besides the immunomagnetic WBC depletion protocols should be considered.

This thesis proposes a technique aimed at WBC depletion of immunomagnetically enriched samples. This technique uses a surface coated with antibodies specifically targeted WBC to capture them and collect a depleted sample containing a higher purity of CTCs. To start, a method was established that can be used to test white blood cell capture under different conditions. Subsequently, the efficiency of capturing white blood cells on the antibody-coated surface was optimised by investigating two types of surface materials and respective coating protocols using enriched and not enriched cell samples. Finally, the enrichment and change in the purity of tumor cells were measured in the remaining sample to evaluate the performance of the white blood cell depletion technique.

To investigate if the proposed technique can overcome the challenges that are faced when processing DLA samples, the main research question should be answered:

“How can an antibody functionalised surface be used to deplete white blood cells from immunomagnetically enriched samples?”

Supporting research questions are:

1. *What factors should be considered to assess the WBC depletion technique?*
2. *How can a surface be coated to deplete immunomagnetically enriched samples?*
3. *What factors affect WBC depletion and CTC collection when processing immunomagnetically enriched samples?*

2.2 ASSESSMENT OF THE TECHNIQUE

Multiple parameters can be used to assess a WBC depletion technique. These factors include the purity of CTCs in the final sample, recovery of CTCs, sample volume that can be processed in a single run, the throughput of sample within a certain time, the scalability of the method and the clinical application. [6,7] Important factors used to assess the technique in this research are the capture efficiency, enrichment, depletion and purity of the produced sample.

Capture efficiency, or yield, quantifies the device's ability to capture WBCs in the sample. This metric is defined as the number of WBCs captured divided by the total number of WBC that were present in the sample. In this research, this is used to evaluate the cell capture on the coated surface.

$$\text{Capture Efficiency} = \frac{(WBC)_{\text{captured}}}{(WBC)_{\text{in}}}$$

Depletion is the inverse of capture efficiency and refers to the factor decrease of WBCs within a volume in the collected sample before and after running the sample through the device being evaluated [27].

$$\text{Depletion} = \frac{(WBC)_{\text{in}}}{(WBC)_{\text{collected}}}$$

Enrichment refers to the factor increase of tumor cells (TCs) within a volume relative to a background of WBCs in the collected sample before and after running the sample through the device being evaluated [6].

$$\text{Enrichment} = \frac{(TCs)_{\text{collected}} / (WBCs)_{\text{collected}}}{(TCs)_{\text{in}} / (WBCs)_{\text{in}}}$$

Purity describes the ability of the device under evaluation to specifically enrich tumor cells or CTCs from a background of WBCs. Purity is defined as the number of CTCs captured divided by the total number of nucleated cells captured [6].

$$\text{Purity} = \frac{(TC)_{\text{collected}}}{(TCs + WBCs)_{\text{collected}}}$$

The number of target cells must be known to assess the efficiency of WBC depletion, CTC enrichment, and purity of a certain technique. This cannot be tested using clinical samples as the actual number of CTCs in a patient sample is always unknown. Instead, cells from cancer cell lines are used [6]. What should be noted is that these cells are different from CTCs. Moreover, the use of cell lines overpredicts the performance of the technique. Cancer cell lines are known to be more homogenous in both their cell surface markers and physical properties and more physically distinct from MNCs than patient CTCs [38].

2.3 ANTIBODY FUNCTIONALISATION OF GLASS- AND HYDROGEL SURFACES

2.3.1 Functionalization of a Hydrogel- and Glass Surface

There exist multiple ways to bind antibodies to a surface. Two of these methods are used in this project. The first method uses salinisation of a glass surface followed by the binding of PEG molecules and the immobilisation of antibodies on the ends of these polymers. The PEG molecules form a two-dimensional, planar structure on which one monolayer of antibodies can be immobilised ($5\text{-}7\text{ ng/mm}^2$) [39,40]. The thickness of the layer depends on the length of the polymer used. The antibody-coated monolayer is expected to be less than 20nm thick [41]. The polymer's length affects the coating's flexibility, which can affect the ability of antibodies to bind to the targeted receptors on the cells [39].

The second method that is used in this project is the functionalisation of a polycarboxylate hydrogel layer (XanTec HC hydrogel slide, XanTec Bioanalytics GmbH, Düsseldorf, Germany) by activation using EDC/NHS chemistry, after which antibodies are bound to the hydrogel. In contrast to the first method, this 1-2 μm thin hydrogel layer contains more antibody binding opportunities due to the many carboxylate groups [39,42]. The schematic image in Figure 2 indicates that multiple antibodies can be bound to the linear polycarboxylate polymers within the hydrogel matrix, enabling 3D immobilisation [43,44]. According to the manufacturer, the hydrogel layer has an immobilisation capacity of $> 50\text{ ng/mm}^2$. The more binding opportunities on the surface, the more antibodies can bind to the surface. This can lead to a higher number of cells captured on the surface.

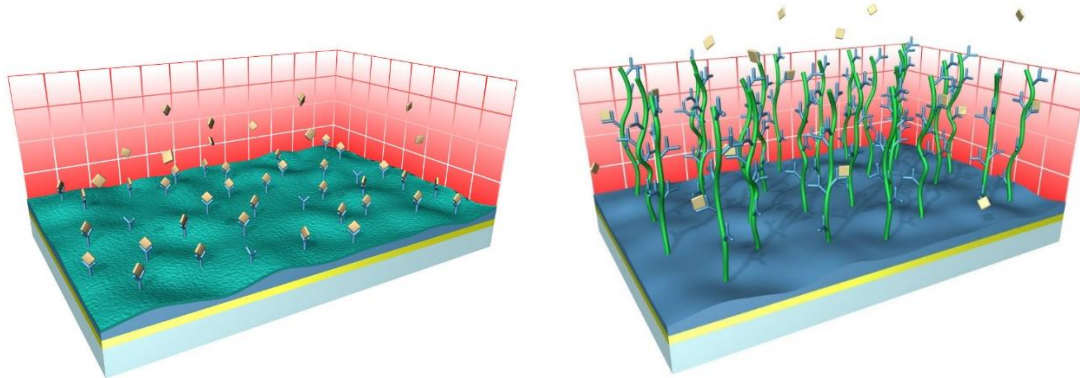


Figure 2 Schematic images of an antibody monolayer on a surface [45] and an antibody-coated hydrogel matrix [43].

Next to that, the flexibility of the hydrophilic polymer chains enables them to align themselves smoothly to the cell surface and allows the receptor molecules to attach at multiple sites simultaneously. The flexibility of the hydrogel matrix is therefore expected to increase cell capture. Besides, the hydrogel matrix is thicker than the PEG monolayer on glass. Coupled with the flexibility of the hydrogel, it is expected that cells can be 'pushed' more into the matrix and contact the matrix with a larger cell surface area, thereby increasing the cell capture on the coated surface.

2.4 CELL CAPTURE

2.4.1 Cell Capture using WBC Specific Antibodies

Antibodies are known for their specific binding to corresponding antigen receptors. The binding affinity of an antibody and targeted antigen differs per chosen antibody-antigen combination and can affect cell capture on a coated surface [46]. The antigen's expression on the cell targeted by the antibody increases the chance that cells will be captured [47]. Therefore, the cell-antibody binding varies per cell type and chosen antibody. To perform WBC depletion of a cell sample containing tumor cells, antibodies specifically targeting these WBCs can be used.

There exist multiple antigens that are expressed in these cells and not in tumor cells. The most common antigen is the CD45 (common leukocyte antigen), a transmembrane glycoprotein expressed on all leukocytes and constitutes about 10% of cell surface antigens [48]. For this reason, antibodies targeting the CD45 receptors of the WBCs are used in this project to specifically bind cells to a surface coated with these antibodies.

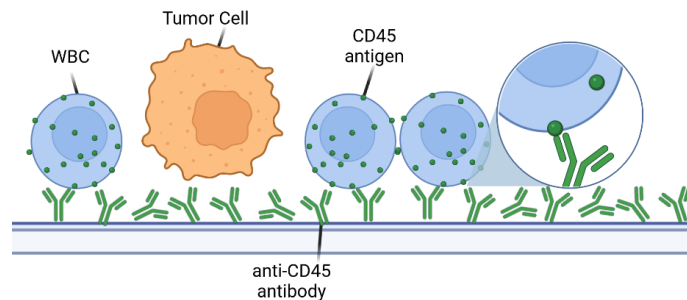


Figure 3 Rough overview of specific binding of WBC-specific antibody anti-CD45. Made with BioRender.

2.4.2 Cell Capture on a Coated Surface and Flow

By flowing a liquid along the coated slide, unattached cells are washed off the slide. The higher the flow speed, the bigger the force, the more cells will be washed off. Depending on the flow speed, cells that are bound to the surface detach and are also washed off the slide. This way, flow speed could affect WBC depletion. At a particular flow speed/force, all cells will detach. Moreover, the flow speed at which cells detach differs between antibody types [46].

2.4.3 Cell Capture on a Coated Surface and Immunomagnetic Enrichment

During immunomagnetic enrichment, ferrofluid nanoparticles modified with anti-EpCAM antibodies bind to the cells. These Fe_3O_4 nanoparticles have a size of 120-200nm [49–51]. Even though these particles target EpCAM-positive cells and not WBCs, WBCs get non-specifically captured during immunomagnetic enrichment. Therefore, the WBCs present in immunomagnetically enriched samples might be bound to immunomagnetic particles. The size of these particles could cause steric hindrance, preventing the WBC-specific anti-CD45 immuno-based capture of WBCs of the proposed WBC depletion technique.

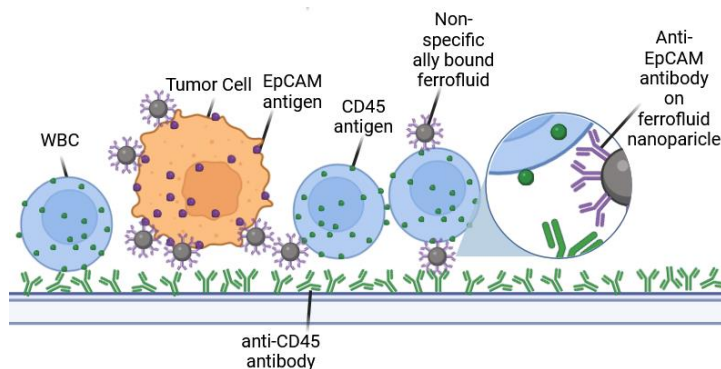


Figure 4 Rough overview of cell capture on a surface of immunomagnetically enriched cells. Anti-EpCAM ferrofluid nanoparticles specifically bind to tumor cells. Some non-specific binding to WBC occurs, possibly preventing specific binding of WBCs to the anti-CD45 antibody-coated surface. Made with BioRender.

2.4.4 Cell Capture on a Coated Surface and Fixed Cells

Clinical samples containing CTCs often have to be preserved for some time before further processing. To prevent sample degradation, it can be stored in preservative tubes containing a fixative [52]. CellSave preservative tubes (Menarini Silicon Biosystems, Bologna, Italy) are clinically used to preserve samples containing CTCs using a mild fixation. This way, samples can be preserved for up to 96 hours, enabling transport of the sample over a long distance [53]. While this can be a great advantage, fixation affects the deformability of cells by creating crosslinks in the cell membrane. While surface proteins can move around freely (to some extent) in live cells, fixation hinders the lateral movement of surface proteins [54,55] (such as CD45). Therefore, it is expected that fixation reduces the binding affinity of cells to an antibody-coated surface.

3.1 SAMPLE PREPARATION

For testing purposes, experiments were initially performed using cell samples that were not immunomagnetically enriched. When a working protocol for white blood cell (WBC) depletion in a multi-well slide was established, immunomagnetically enriched samples were used for WBC depletion. Cells from lymphocyte- and prostate cancer cell lines have been used as well as MNC isolated from healthy donor blood to resemble a DLA sample better.

3.1.1 Cell Culture

Initial testing of cell capture on the coated surface was performed using lymphoblastoid cell line LCL, and prostate cancer cell lines LNCaP and PC3. PC3 and LNCaP cell lines were cultured in RPMI 1640 medium with L-Glutamine (Lonza, Basel, Switzerland), 10% FBS (Sigma-Aldrich, St. Louis, MO, USA) and 1% penicillin/streptomycin (Lonza, Basel, Switzerland). LCL cells were cultured in RPMI 1640 medium with L-Glutamine, 15% FBS and 1% penicillin/streptomycin.

3.1.2 Healthy Donor Blood Samples

Blood samples were collected in CellSave preservative tubes (Menarini Silicon Biosystems, Bologna, Italy) from healthy anonymised donors at the University of Twente ECTM donor service. Written consent was obtained from all donors. WBCs were isolated from whole blood samples obtained from healthy donors. To better represent a DLA sample, WBC isolation was performed via a density separation targeting MNCs using Ficoll-Paque PLUS with a density of 1.077 ± 0.001 g/mL (GE Healthcare, Hoevelaken, Netherlands). This way, the mononuclear cell fraction i.e. lymphocytes and monocytes could be isolated from the blood sample.

3.1.3 Antigen Expression

The cell capture of white blood cells to the anti-CD45 antibody-coated surface is expected to depend on the expression of the CD45 antigen on the white blood cells. To find out if the cell types that were used expressed the CD45 antigen, anti-CD45 antibodies were allowed to bind to the cells. Subsequently, the cells were stained with goat anti-mouse IgG-PE (0.5 μ g/mL) (Sigma-Aldrich, St. Louis, USA) which binds to the anti-CD45 antibodies. Additionally, the EpCAM expression of PC3 cells was measured to determine if cell capture on the coated surface is related to antigen expression. The PC3 cells were stained with VU1D9-PE which binds to EpCAM. Quatibrite-phycoerythrin (PE) beads (BD Biosciences) were then used to quantify the expression of CD45 or EpCAM on these cells. The EpCAM expression of LNCaP cells was previously measured by the research group.

3.1.4 Fluorescent Staining of Cell Sample

To be able to visualise the cells on the coated surface, LCL cells and WBC from blood were fluorescently stained with Hoechst (Hoechst 33342, ThermoFisher Scientific, Waltham, MA, USA) and PC3 and LNCaP cells were fluorescently stained with CellTracker Orange (CTO) (Thermo Fisher Scientific, Waltham, MA, USA) before adding the cell sample to the surface. A standard curve was created using different amounts of fluorescently stained cells to relate the fluorescence intensity to the number of cells present on the surface/in a well. For WBC depletion experiments involving LCL and PC3 cells, these cells are used in a 10:1 ratio with 110 thousand cells per well. Therefore, the standard curve for LCL cells was made using 1 to 150 thousand cells per well.

3.1.5 Fixation

Initial experiments were performed using live cells as well as fixed cells. For fixation, cells were preserved in CellSave Preservative Tubes (Menarini Silicon Biosystems, Bologna, Italy), which are generally used to stabilise CTCs for up to 96 hours at RT. Cells were fixated and stored at room temperature for at least one day before the depletion experiments.

3.1.6 Immunomagnetic Enrichment

To perform immunomagnetic enrichment, PC3 cells were spiked into a sample containing LCL cells or WBC isolated from healthy donor blood. This sample was then supplemented with casein buffer to prevent non-specific binding. CellSearch ferrofluid (Menarini Silicon Biosystems, Bologna, Italy) was added to the mixture at a final concentration of 3.3 $\mu\text{g}/\text{mL}$, followed by a 3-minute incubation period. To minimise cell aggregation, 20 $\mu\text{g}/\text{mL}$ Desoxyribonuclease (DNase) and 20 mM magnesium sulfate (MgSO_4) were added, followed by another 3-minute incubation period. Capture enhancement (Menarini Silicon Biosystems), containing streptavidin, was then added to the sample at the same volume as the iron particles to enhance the capture of tumor cells. The mixture was placed in a BD iMag Cell Separation magnet (BD, Franklin Lakes, NJ, USA) and subjected to 7 cycles of 3 minutes of magnetic incubation. Samples were mixed in between. Subsequently, the sample tubes were secured to the magnet using tape, and after 10 minutes the supernatant was gently aspirated using a syringe pump at 2 mL/min. Immediately after aspirating, 1 mL of casein buffer was added to the sample tube. After adding this buffer and mixing the sample, another 10-minute magnetic incubation step was performed, followed by gentle aspiration of the supernatant (2 mL/min). The cells were then resuspended in 500 mL casein buffer. Biotin was added to the mixture to counteract the effect of desbiotin on the ferrofluid. After a waiting period of 5 minutes and mixing the sample, the sample was ready for further processing.

3.2 EXPERIMENTAL SETUP

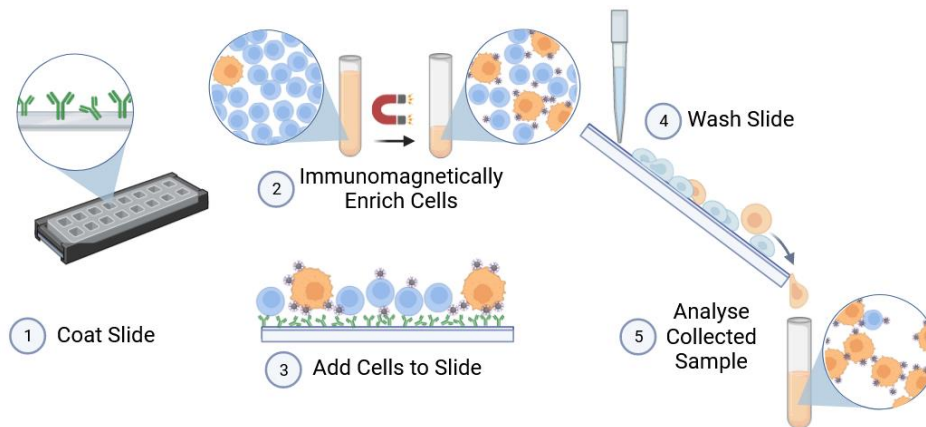


Figure 5 Steps to test WBC depletion of an immunomagnetically enriched sample on an antibody-coated slide: 1. A multi-well slide holder with glass- or hydrogel layer slide was used to create wells. The slide was then coated with antibodies. 2. The sample was prepared by immunomagnetic enrichment. 3. The sample was added to the wells and the slide was centrifuged. 4. The slide was washed to remove unbound cells and collect them. 5. The sample containing the washed off cells was analysed. Made with BioRender.

To observe the cell capture on a coated surface, a multi-well slide adapter was placed on top of glass microscope slides, creating a multi-well slide with wells of $7 \times 7 \text{mm}^2$ that can be imaged under a microscope. This way, it was possible to observe the cells throughout the experiment. The surface area inside each well could be treated independently, making it possible to test various conditions on one microscope slide. In this research, the multi-well slide setup was used to test and optimise the technique. Ultimately, the coated surface should be large enough and shaped to increase the amount of sample that can be processed. A simplified overview of the testing process is shown in Figure 5. After the surface was coated with antibodies, an (immunomagnetically enriched) cell sample could be added to the surface. The cells were allowed to bind to the surface, after which the slide was washed and the unbound, washed off cells were collected. The collected sample could then be analysed.

3.3 SURFACE MODIFICATION

Two types of surfaces were coated with anti-CD45 antibodies to capture white blood cells; a glass surface and a glass surface with a hydrogel layer. The coating was performed using a different protocol for each surface type. Initially, experiments were performed using a glass surface. Later, the antibody coating of a hydrogel layer was tested as well. As both surfaces and corresponding modifications could adhere antibodies to the surface that remained present after multiple washing steps, it was chosen to continue with both surface modification protocols for further testing.

3.3.1 Antibody Coating of a Glass Surface

Initially, glass slides were treated with Piranha (7:3 sulfuric acid and 35% hydrogen peroxide) for 20 minutes to create hydroxyl groups, after which the slides were washed with MQ (Milli-Q water) and ethanol. Next, a coating of (3-aminopropyl)triethoxysilane (APTES) (Sigma-Aldrich, St. Louis, USA) was applied for salinisation by immersing the slides in an ethanol solution containing 0.005M APTES and incubating them at 37°C for 4 hours. The slides were then washed with ethanol, dried and stored at 4°C till further use. Two days before adding the cell sample, one of the slides was placed in a multi-well slide holder (Grace Bio-labs, Bend, U.S.A.) to create a wells plate. The slide was treated with polyethylene glycol diglycidyl ether (PEG diglycidyl ether, Mn 500) (Sigma-Aldrich, St. Louis, USA) overnight at 50°C. Afterwards, the slide was washed using ethanol, followed by MQ to remove excess PEG and the slide holder was reattached. Subsequently, the slide was coated with antibodies by dissolving anti-CD45 antibody (HI30) (manufacturer unknown) in 2M HNa2PO4 (pH-9) and incubating at 4°C overnight. After blocking with PBS/BSA (1%), the slide was washed two times and ready for further processing.

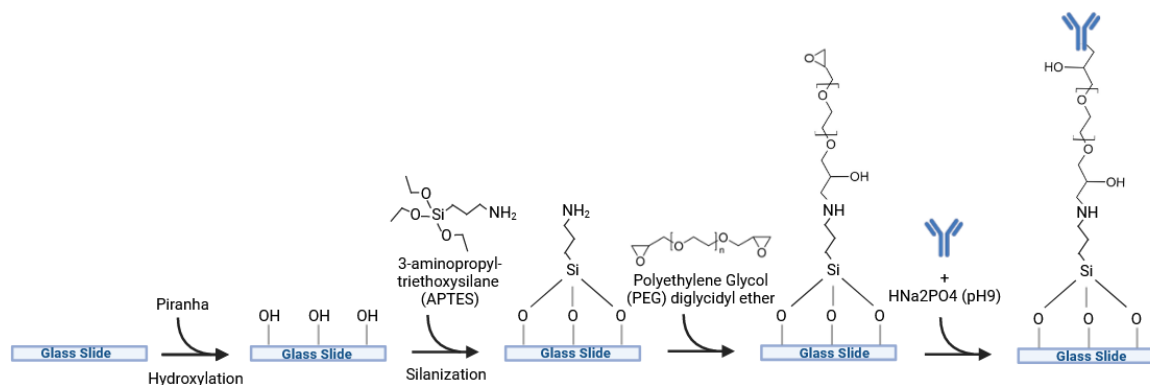


Figure 6 Schematic protocol for antibody immobilisation of the glass surface, made with BioRender.

3.3.2 Antibody Coating of a Hydrogel Layer

A polycarboxylate hydrogel-coated glass slide (HC 1500nm) (XanTec Bioanalytics GmbH, Dusseldorf, Germany) was taken and a multi-well slide holder (Grace Bio-labs) was attached to create wells. Each well was filled with MQ and the slide was incubated at room temperature (RT) for 15 minutes. Next, the slide was treated with EDC/NHS (1:1 EDC (400 mM) and NHS (100 mM)). The slide was incubated for 30 minutes at RT to allow for the activation of the hydrogel coating. Afterwards, the slide was washed using a 5 mM acetic acid solution. The anti-CD45 (HI30) antibody (manufacturer unknown) was dissolved in sodium acetate buffer (5 mM) to achieve the desired antibody concentration. The slide was incubated in the antibody solution for 1 hour at RT. Wells were washed with MQ to remove unbound antibodies. Unoccupied binding sites were blocked by adding ethanolamine blocking solution (1 M, pH 8.5) to the wells and incubating for 30 minutes at RT. Finally, the wells were washed two times with PBS (Phosphate Buffered Saline) before further processing.

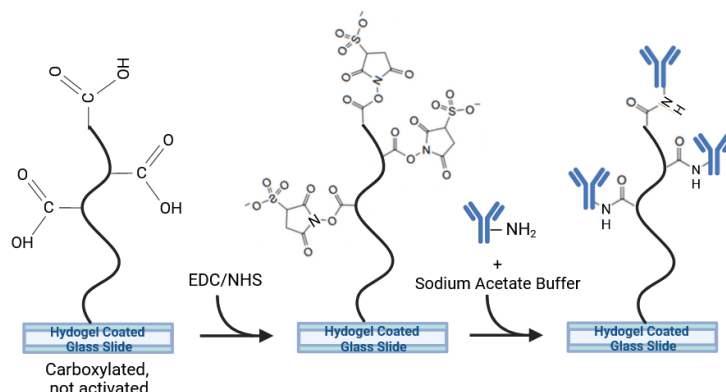


Figure 7 Schematic protocol for antibody immobilisation of the hydrogel layer, made with BioRender.

3.3.3 Visualisation of the anti-CD45 Antibody Coating

A titration was performed to identify the antibody concentration that resulted in the highest coating density. For this, a glass slide/hydrogel slide was coated, after which the coated antibody was stained using goat anti-mouse

IgG-PE (0.5 µg/mL) (Sigma-Aldrich, St. Louis, USA) in PBS/BSA (1%). The slide was incubated with the staining solution for 15 minutes at RT. Wells were washed twice with PBS/BSA (1%) to remove the excess staining solution. Subsequently, the slide was scanned using a Nikon Ti-E inverted microscope (Nikon Instruments, Melville, USA), capturing images of the whole slide in the PE channel to visualise the antibody coating. The slide was scanned again after multiple additional washing steps to test if the coating was still present after washing. The mean fluorescence intensity in a well was measured before- and after washing steps using ImageJ software (U.S. National Institutes of Health, Bethesda, USA). To compare the different antibody concentrations on the coating, the mean fluorescence intensity of the coated wells was normalised to the mean intensity of an uncoated well.

3.4 CELL CAPTURE ON THE COATED SURFACE

3.4.1 Cell Capture on the Antibody-Coated Surface in the Multi-well Slide

After coating the slide with anti-CD45 antibodies, a sample containing the desired amount of fluorescently stained WBC from healthy donor blood or LCL cells and LNCaP or PC3 cells was added to each well of the created multiwell slide. The slide was centrifuged for 5 minutes at 1000 rcf (relative centrifugal force) to promote cell attachment. The slide was scanned using a Nikon Ti-E inverted microscope (Nikon Instruments, Melville, USA), capturing images of the whole slide in the PE and DAPI channels with a 4x objective. Each well was washed twice with 100 µL of PBS/BSA (1%) using a micropipette. When desired, the removed liquid was collected in a separate tube for subsequent FACS analysis. After washing, the slide was scanned using the Nikon Ti-E inverted microscope, using the same settings. Then, the multiwell holder was removed, and the slide was washed using a 1000 µL micropipette by pipetting 6 times 1 mL PBS/BSA (1%) onto one end of the angled slide, allowing it to flow over the slide (with the coated side facing upward or downward). A cover glass was carefully attached to the slide and the whole slide was imaged again using the same settings.

3.4.2 Statistical Analysis

Differences between groups as a result of a single factor were tested using independent (unpaired) T-tests. If the assumption of homogeneity of variance was not met according to Levene's test for equality of variance ($p < 0.05$), Welch's T-test was used to determine significance. All statistical tests were two-sided with $P < 0.05$ considered as statistically significant. To compare the effect of multiple factors, ANOVA was used.

3.5 IMAGE ACQUISITION AND ANALYSIS

3.5.1 Fluorescence Imaging

A Nikon Ti-E inverted microscope (Nikon Instruments, Melville, USA) with Nikon Ti-E scanning software was used to scan the slides in the PE and DAPI channels to image the cells on the slide. The entire slide was imaged with a 4x objective, using an exposure time of 100ms and 200ms for DAPI and PE respectively. These images were later put together into a montage of the whole slide using the software program ImageJ (U.S. National Institutes of Health, Bethesda, USA) and further processed using the software program Hokawo (Hamamatsu Photonics Deutschland GmbH, Herrsching am Ammersee, Germany) to make an overlay of the DAPI and PE images. The same settings were used for making overlay images of all experiments.

3.5.2 Quantification of the Fluorescent signal

The software program ImageJ was used to measure the mean fluorescence intensity of selected ROIs within the montage images of the scanned slides. Depending on the experiment, an ROI containing an entire well or a smaller ROI was used. Multiple ROIs were measured in the DAPI and PE channels for each condition tested on a slide. The mean fluorescence intensity within an ROI was measured before and after the washing steps. This was done separately for the DAPI and PE channels. Next, the percentage of mean fluorescence intensity left in the ROI after the washing steps was calculated to determine the cell capture percentage on the surface. To normalise the data to the background signal, the mean fluorescence of an ROI where no cells were visible or an ROI within an empty well was measured and subtracted from the other measurements. Then, the average cell capture percentage was calculated for each condition that was tested in the experiment. Instead of analysing the whole well, it was later in the project chosen to analyse cell capture in subsequent experiments in 6 different ROIs of 3x3mm² per condition. This was to reduce the variation between wells caused by debris in the liquid or bubbles under the coverslip.

3.6 TUMOR CELL RECOVERY OF THE DEPLETED SAMPLE

3.6.1 Analysis of the Collected Sample

As mentioned in 3.4.1, the liquid used for washing - which represents the depleted sample - could be collected in a separate tube. To evaluate WBC depletion and CTC recovery, the recovery of each cell population was counted using flow cytometry (BD FACS Aria II). The instrument was calibrated using CS&T beads (BD) before use. For cell identification, PC3 cells were stained with CTO and both PC3 and LCL cells were stained with Hoechst. Gates were placed to indicate the cell population in the forward- and side scatter plot. Within this population the Hoechst positive and CTO negative cells were indicated as LCL cells. The Hoechst positive and CTO positive cells were indicated as PC3 cells. These gates were set in the DAPI and PE scatterplot. The ratio of LCL and PC3 cells was calculated before and after depletion on the coated surface by measuring 10 thousand events per sample. To be able to make a comparison of the coated glass- and hydrogel slide, the same volume and therefore same number of cells was added to the respective surface type. In addition to this, the collected sample of a depleted, CellSave (Menarini Silicon Biosystems, Bologna, Italy) fixed, immunomagnetically enriched sample containing PC3 cells and MNCs isolated from a healthy donor blood sample was prepared. Prior to immunomagnetic enrichment, 50 thousand PC3 cells were spiked in a sample containing 20 million MNC cells.

3.6.2 Flow Channel Setup for Collection of The Depleted Sample

To be able to control the flow speed that is used for washing the unbound cells off the coated surface, a 6-channel bottomless sticky slide (ibidi, Gräfelfing, Germany) was attached to the coated surface of a microscope glass, creating six 3.8 mm wide, 17 mm long and 0.4 mm high flow channels. After pipetting a cell sample in each flow channel, the slide was centrifuged for 5 minutes at 1000 rcf to promote cell attachment. After scanning, a syringe pump equipped with a syringe containing PBS/BSA (1%) to was attached to the inlet of the flow chamber. During flow the slide was placed onto a Nikon Ti-E inverted microscope, visualising the cells in the flow channels in real-time. The liquid pushed through each channel could be collected for subsequent FACS analysis.

4

RESULTS

4.1 ESTABLISHMENT OF A WHITE BLOOD CELL DEPLETION TECHNIQUE

4.1.1 Glass Surface Coating

As can be seen in Figure 8, the mean fluorescence ratio that is measured in wells that have been coated varies depending on the anti-CD45 concentration. The shape of the graph shows that the highest fluorescence intensity is reached using 20 $\mu\text{g}/\text{mL}$ anti-CD45 and decreases at 60 $\mu\text{g}/\text{mL}$. This could indicate a peak value for the antibody concentration used for coating the surface, which probably lies between 20 and 60 $\mu\text{g}/\text{mL}$. However, this has not been tested. Following the results of this experiment, it was decided to proceed with a concentration of 20 $\mu\text{g}/\text{mL}$ for coating on a glass surface. In addition, a structure can be observed in the images in Figure 8. The crystallisation of HNaPO_4 presumably causes this structure during the coating process.

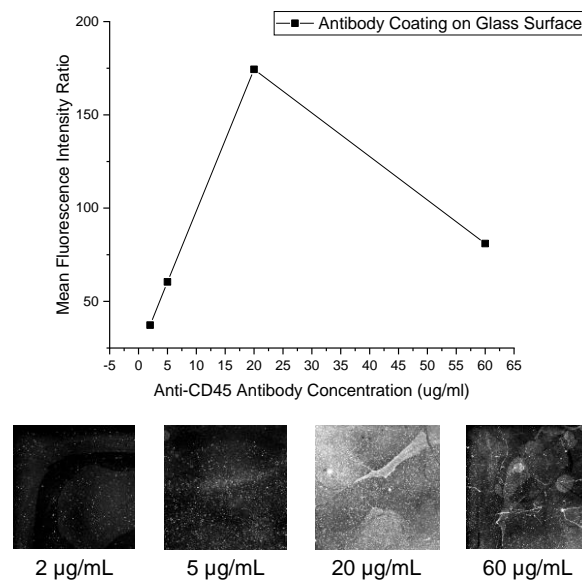


Figure 8 Mean Fluorescence intensity ratio of goat anti-mouse IgG-PE bound to the anti-CD45 antibody coating on a glass surface after washing steps for different concentrations of anti-CD45 antibody and images of $3.5 \times 3.5 \text{mm}^2$ of the coated slide.

4.1.2 Hydrogel Surface Coating

When testing the coating on a hydrogel layer using the same antibody concentrations, no plateau or peak value was found in this experiment (Appendix 7.1). Therefore, higher concentrations were tested (Figure 9). This graph and the corresponding images indicate that 120 $\mu\text{g}/\text{mL}$ results in the highest fluorescence intensity ratio of all tested concentrations. Therefore, further experiments were performed using this concentration. Assessing the shape of the graph, the antibody concentration resulting in the most antibodies bound to the surface may be slightly higher than 120 $\mu\text{g}/\text{mL}$.

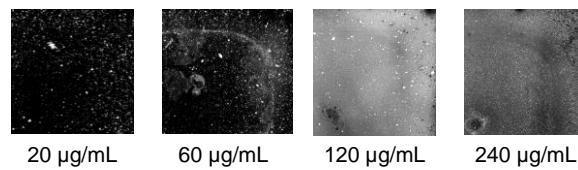
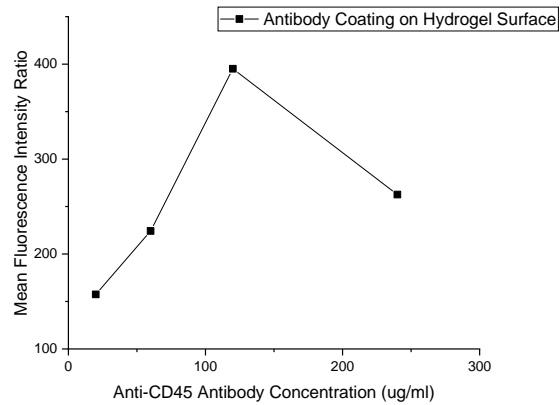


Figure 9 Mean Fluorescence intensity ratio of goat anti-mouse IgG-PE bound to the anti-CD45 antibody coating on a hydrogel surface after washing steps for different concentrations of anti-CD45 antibody and images of 3.5x3.5mm² of the coated slide.

The images of the coating on the hydrogel layer show a more even distribution of antibodies compared to the coating on the glass surface. Next to that, the antibody concentration used for the coating on the hydrogel layer is six times higher than the concentration used on the glass surface. This could indicate that more antibodies can be bound on the hydrogel layer which could in turn lead to a higher cell capture on the surface. To investigate this, the cell capture on the surface is tested on both surface types.

4.1.3 Fluorescence Intensity and Cell Count

A standard curve was made to quantify the cell capture on the surface plotting the mean fluorescence intensity in a well against the number of stained cells in that well. Figure 10 shows these plots for LCL cells stained with Hoechst (MFI = 0,0242 · N_{Cells} + 574,91) and PC3 cells stained with CTO (MFI = 0,0533 · N_{Cells} + 236,11). A linear relationship is found in both curves with R² values close to one. Assuming that the fluorescence intensity is similar in each experiment, the number of LCL or PC3 cells in a ROI can be calculated from the fluorescence intensity.

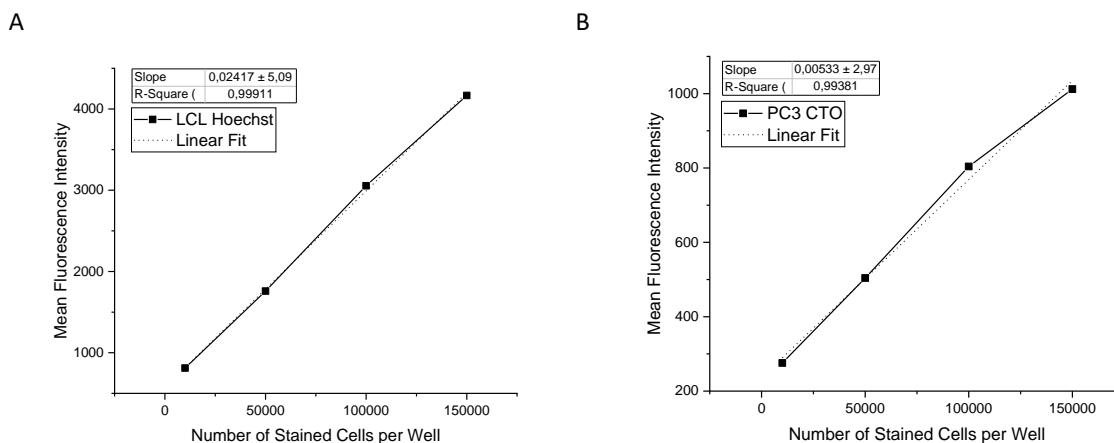


Figure 10 (A) Mean fluorescence intensity and number of Hoechst stained LCL cells per well. (B) Mean fluorescence intensity and number of CTO stained PC3 cells per well.

4.1.4 Antigen Expression

The BD Quantibrite Beads assay results are presented in Table 1 and show the expression of CD45 and EpCAM antigens of the cell types used. As expected, the calculated amount of antibodies bound per cell indicates that PC3 cells express near zero CD45 compared to LCL cells. The CD45 expression of the mononuclear cell fraction (MNC) isolated from healthy donor blood is higher compared to the LCL cells. LNCaP cells have a high expression of EpCAM compared to PC3 cells.

Table 1 Antigen expression of EpCAM and CD45 of PC3, LNCaP, LCL and MNC from healthy donor blood measured using BD Quantibrite Beads.

| ANTIBODY BOUND PER CELL | CELL TYPE |
|-------------------------|------------------------------|
| EpCAM | |
| 600.000 | LNCaP |
| 14.379 | PC3 |
| CD45 | |
| 33.509 | LCL |
| 44.237 | MNC from healthy donor blood |
| 283 | PC3 |

4.1.5 Isolation of MNC from Whole Blood

As shown in Figure 11, the mononuclear cell fraction (MNC) isolated from a whole blood sample of a healthy donor include evident populations of lymphocytes and monocytes. There are few granulocytes in this sample, as no clear population is visible in the scatterplot. These isolated cells were later used instead of LCL cells to prepare a sample that better resembles a DLA sample.

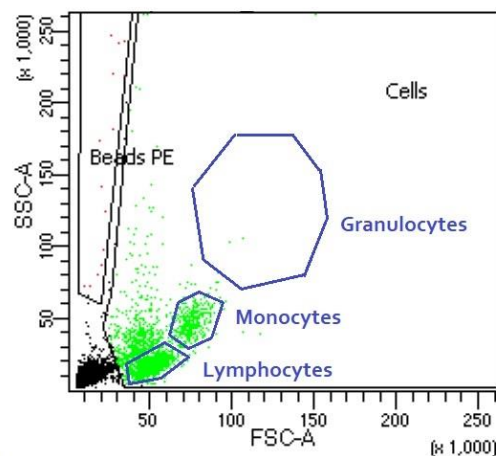


Figure 11 Forward- and side scatter plot of white blood cells isolated from healthy donor blood sample. Lymphocyte and monocyte and granulocyte populations are indicated by a blue gate. There is no clear granulocyte population visible in this sample.

4.1.6 Cell Capture on the Antibody-Coated Surface

Cell Capture of LCL or LNCaP Cells on an anti-CD45- or VU1D9 Coated Glass Surface

Figure 12 Images of fluorescently stained LCL or LNCaP cells on a glass slide coated with anti-CD45 antibodies (20 µg/mL) or VU1D9 (20 µg/mL) respectively, before- and after washing steps. Images are taken of the whole well to visualise the distribution of cells inside the well. As CD45 is expressed on LCL cells, it was expected that the anti-CD45 coated surface could capture these cells. Figure 12 shows that LCL cells (66%) remained on the surface of the antibody-coated well after washing and not (1%) in the well without antibodies. As EpCAM is highly expressed on LNCaP cells, it was expected that the VU1D9 coated surface would be able to capture these cells. As seen in Figure 12, most of the LNCaP cells (90%) remain present after washing steps and are evenly distributed throughout the whole surface area. In the well without antibodies only 25% of all cells remain present after washing steps and the cells are distributed along the edges and are not located in the centre of the well.

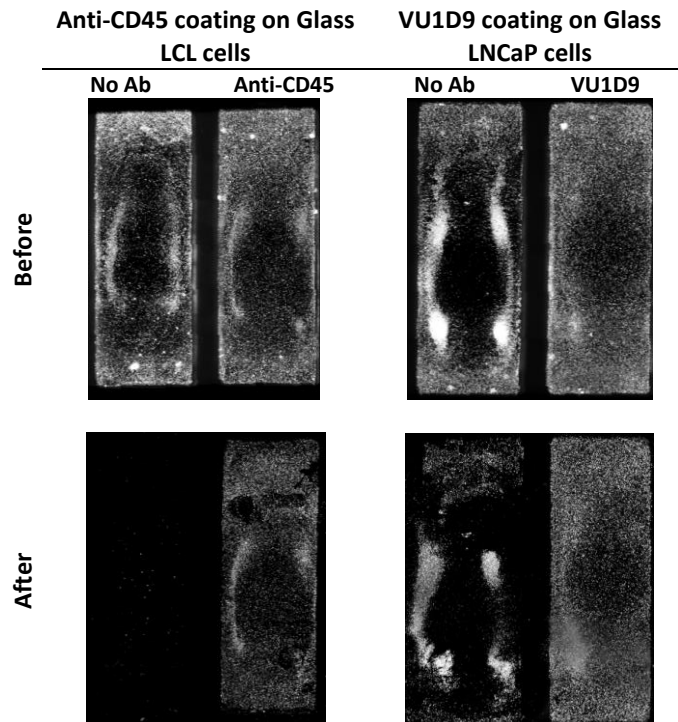


Figure 12 Images of fluorescently stained LCL or LNCaP cells on a glass slide coated with anti-CD45 antibodies (20 $\mu\text{g}/\text{mL}$) or VU1D9 (20 $\mu\text{g}/\text{mL}$) respectively, before- and after washing steps. Images are taken of the whole well to visualise the distribution of cells inside the well.

Cell Capture of LCL or LNCaP Cells on an anti-CD45- or VU1D9 Coated Hydrogel Surface

Antibody coating on a hydrogel surface was tested using anti-CD45 antibodies and LCL cells as well as VU1D9 antibodies and LNCaP cells. What can be seen in Figure 13 is that only a small portion (5%) of the LCL cells is captured on the anti-CD45 antibody-coated surface and no cells (< 1%) were captured on the surface without antibodies. The cell capture of LNCaP cells on a (VU1D9-coated) hydrogel surface was 65% with antibodies and 8% without antibodies. Similar to the observations that were made of the glass surface, the targeted cells are less evenly distributed in the wells without antibodies. Even though the images in Figure 13 indicate that the coating on a hydrogel surface is able to capture cells, the cell capture is less evident when using anti-CD45 antibodies. This might be due to a difference in binding affinity or antigen expression of the respective cell type and antibody. Further in the project, the cell capture using other antibody concentrations was tested.

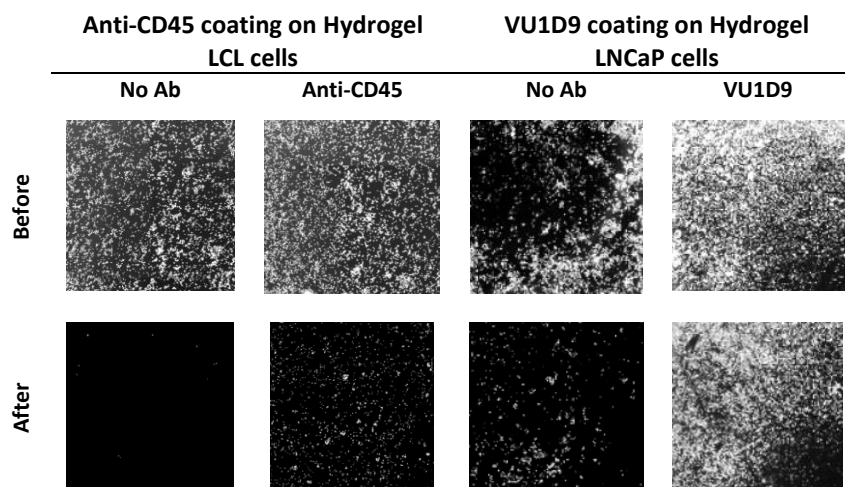


Figure 13 Images of fluorescently stained LCL or LNCaP cells on a hydrogel layer coated with anti-CD45 (20 $\mu\text{g}/\text{mL}$) or VU1D9 antibodies (20 $\mu\text{g}/\text{mL}$) respectively, before- and after washing steps.

Cell Capture and EpCAM Antigen Expression

It was tested if the cell capture on the coated surface is related to the expression of the targeted antigen on the cell. Two prostate cancer cell lines were chosen that have a relatively similar cell size but differ in EpCAM expression (see Table 1); PC3 (16.6 μm) and LNCaP (18 μm). It can be seen from the images in Figure 14 that capture of PC3 cells - which have a relatively low EpCAM expression – on the coated surface is low (7%) in comparison to the capture of LNCaP cells (45%) which have a high expression of EpCAM. What should be noted is that this is half of the cell capture percentage that was measured in previous experiments. Only 1% of cells remained present in wells that were not coated with antibodies. The images in Figure 14 show that LNCaP cells are evenly distributed on the surface and PC3 cells are not. Instead, the cells seem to be in clumps which could have caused them to be washed away more easily. This clumping might result from too high confluency in the cell culture flask.

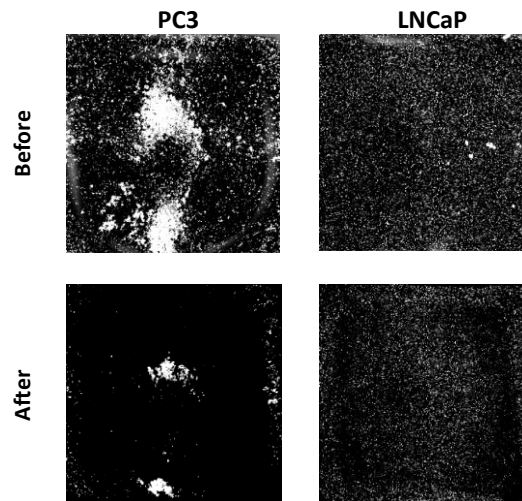


Figure 14 Images of a glass surface coated with VU1D9 antibodies (20 $\mu\text{g}/\text{mL}$) with two types of fluorescently stained tumor cells: PC3 (low EpCAM expression) and LNCaP (high EpCAM expression). Images of cells on the surface before- and after washing steps in a whole well. This experiment was performed from surface modification to imaging at two separate times.

Specific and Non-Specific Cell Capture of PC3 and LCL Cells

To further demonstrate this, the capture of LCL- and PC3 cells was tested in separate wells on a glass- and hydrogel slide that was coated with anti-CD45 or VU1D9 antibodies or without antibodies. This allows the measurement of specific and non-specific binding of each cell type. The cell capture was measured in six separate ROIs for each of these conditions and is presented in the graph in Figure 15.

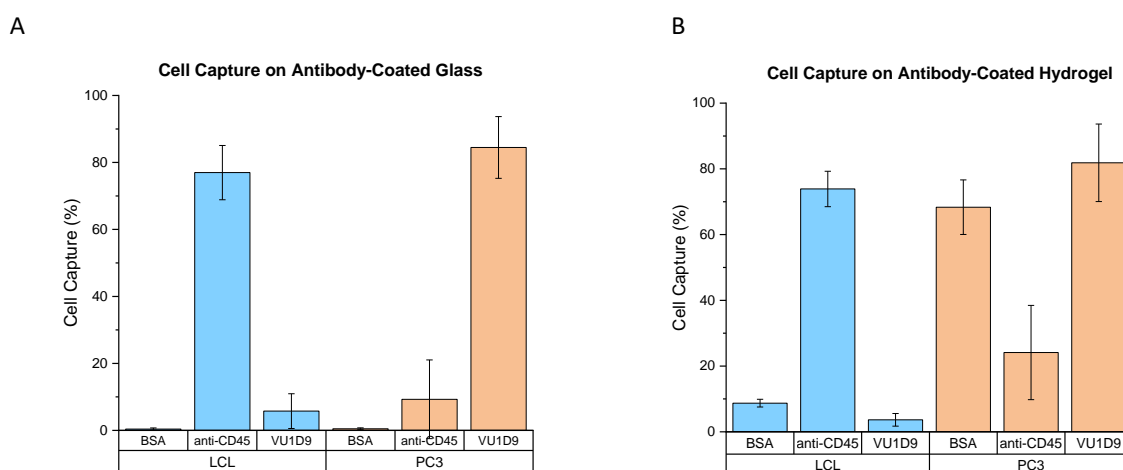


Figure 15 Cell capture percentage of LCL and PC3 cells after washing on an antibody-coated glass- and hydrogel surface. The surface was coated with anti-CD45 (20 $\mu\text{g}/\text{mL}$ on glass, 120 $\mu\text{g}/\text{mL}$ on hydrogel), VU1D9 (20 $\mu\text{g}/\text{mL}$ on glass, 120 $\mu\text{g}/\text{mL}$ on hydrogel) or no antibody (BSA). The mean fluorescence intensity of six individual ROIs of 3x3mm² was measured for each condition.

The measured cell capture percentage is near 80% for the targeted cell type of each antibody on both surfaces. On glass (Figure 15A), the cell capture is near zero on the surface without antibodies (only BSA) for each cell type. There is however non-specific cell capture of LCL cells on the VU1D9 coated surface and of PC3 cells on the anti-CD45 coated surface. What should be noted is that the standard deviation of the non-specific capture is relatively high. This might be explained by the uneven spread of non-targeted cells that is previously mentioned. On hydrogel (Figure 15B), the non-specific binding of PC3 cells on the anti-CD45 coated surface (24%) is higher compared to the glass surface (9%). However, this difference is not significant based on this data because of the large standard deviation and the fact that the data is not normally distributed (Shapiro-Wilk). On the other hand, the non-specific cell capture on the hydrogel surface without antibodies is clearly higher compared to the glass surface for both the LCL (9%) and PC3 (68%) cells (Welch's T-test, $p < 0.001$). A possible explanation for this could be that BSA might be a better blocking agent than ethanolamine, as BSA was only briefly added to the hydrogel surface in this experiment. Moreover, the non-specific binding is lower for each cell type on the antibody-coated surface versus the surface without antibodies, which could result from the antibodies already occupying the binding sites that therefore do not need to be blocked. Next to that, the data in Figure 15 indicates that the non-specific binding of PC3 cells is higher compared to LCL cells which is evident on the hydrogel surface without antibodies (Welch's T-test, $p < 0.001$) but is less apparent on the antibody-coated glass- and hydrogel surface.

4.1.7 Antibody Concentration and Cell Capture After Washing Steps

In addition to finding the highest coating density, the cell capture on the coated glass- and hydrogel surface dependent on the antibody concentration was assessed using a titration. Cells were added to the surface of a $7 \times 7 \text{ mm}^2$ well in a 10:1 ratio, with a total of 110 thousand cells per well. This was chosen to prevent wells from becoming overcrowded and cells not having the opportunity to bind to the surface. In theory, this is approximately 33% of the number of cells that would fit on the surface, provided that LCL cells have a diameter of $13 \mu\text{m}$ and PC3 cells have a diameter of $16.6 \mu\text{m}$.

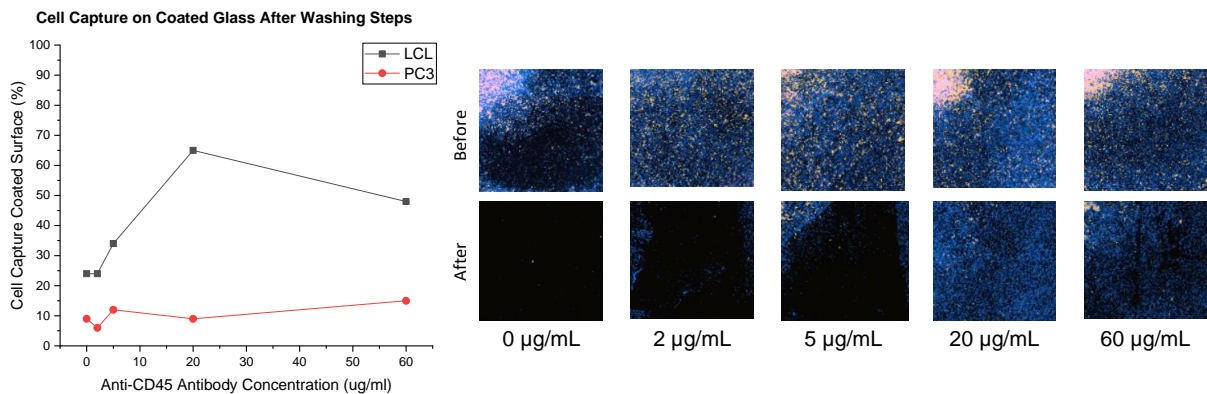


Figure 16 Cell capture on a coated glass surface for different concentrations of anti-CD45 antibodies, measured by the percentage of mean fluorescence intensity of a well before- and after washing steps. Images of the LCL (Blue) and PC3 (Orange) cells on the coated slide ($3 \times 3 \text{ mm}^2$, corner of a well).

The graph in Figure 16 shows the cell capture percentage in wells that were treated with different antibody concentrations. It shows that for an antibody concentration of $20 \mu\text{g/mL}$ and higher, more than half of the LCL cells are captured on the surface, and nearly 90% of the PC3 cells are washed off of the surface. In the corresponding images it can be observed that for a higher antibody concentration, LCL cells are more evenly distributed on the surface. In contrast, PC3 cells seem to accumulate in the middle (top left in each image) of the well.

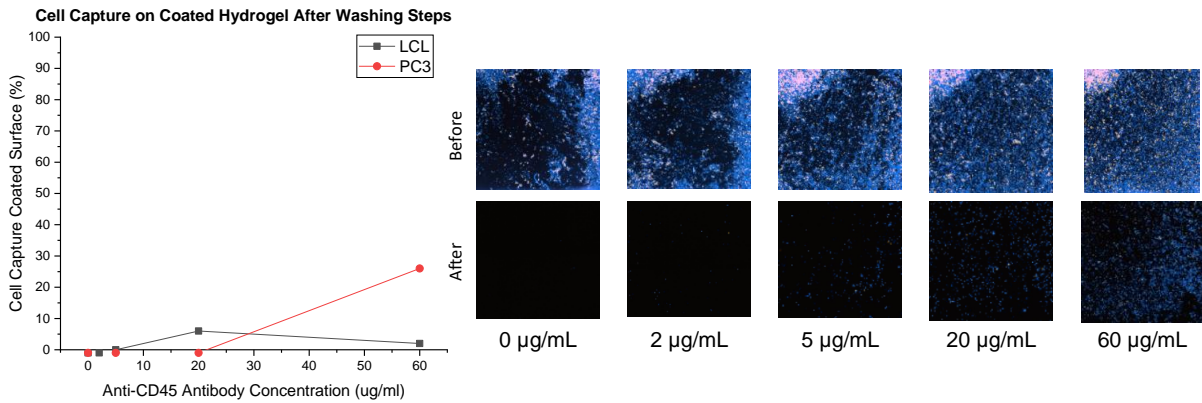


Figure 17 Cell capture on a coated hydrogel surface for different concentrations of anti-CD45 antibodies, measured by the percentage of mean fluorescence intensity of a well before- and after washing steps. (images: LCL (Blue) and PC3 (Orange))

The graph and images in Figure 17 show the cell capture on the coated hydrogel surface. It is apparent that with an increasing concentration of antibodies on the surface, the cell capture on the surface after the washing steps increases as well. However, for an antibody concentration of 60 µg/mL the cell capture is very low (< 10%). To find the most suitable antibody concentration to use on the hydrogel, it was chosen to repeat this experiment with even higher concentrations of antibodies on the surface (Figure 18).

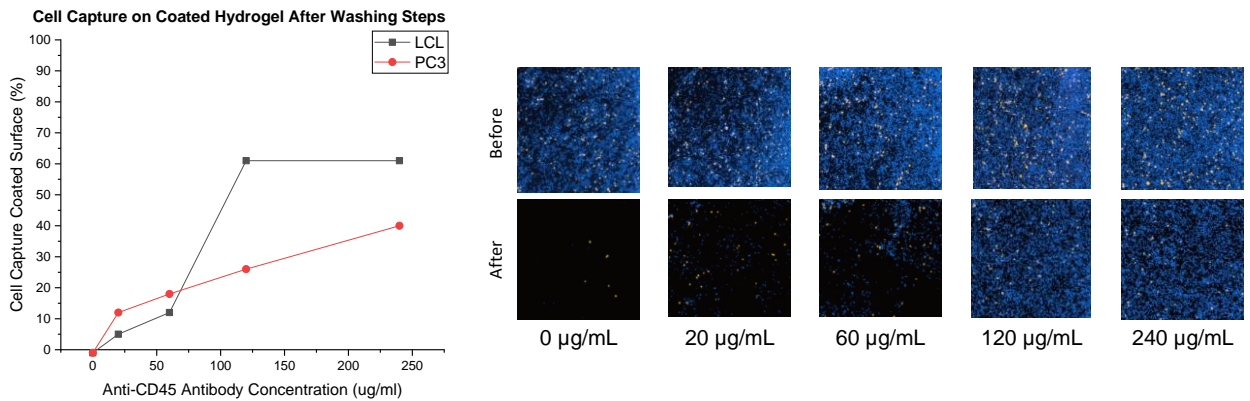


Figure 18 Cell capture on a coated hydrogel surface for different concentrations of anti-CD45 antibodies, measured by the percentage of mean fluorescence intensity before- and after washing steps. (images: LCL (Blue) and PC3 (Orange))

For an antibody concentration of 120 µg/mL or 240 µg/mL there is no apparent difference between the cell capture of LCL cells on the surface. The capture of PC3 cells on the surface is higher for an antibody concentration of 240 µg/mL than for 120 µg/mL. Therefore, it seems unnecessary to use twice the amount of antibody to capture the same amount of LCL cells. Next to that, the unwanted capture of PC3 cells increases at higher concentrations. As a result, it was chosen to perform further experiments using the hydrogel surface with an antibody concentration of 120 µg/mL.

Comparing the measured cell capture of the glass- and hydrogel surface for the chosen antibody concentration, it seems to be relatively equal for the LCL cells (65% and 61%, respectively) but different for the PC3 cells (9% and 26%). Based on this data and the fact that only one-sixth of the antibody concentration is needed, the coated glass surface might be more suitable for WBC depletion.

4.2 EFFICIENCY OF WHITE BLOOD CELL DEPLETION ON A MULTIWELL SLIDE

The efficiency of white blood cell depletion on the coated multi-well slide was first investigated by measuring the cell capture on the coated surface. Differences in cell capture were investigated for a variation in samples and surfaces.

4.2.1 Washing Steps

The cell capture percentage was measured on four independent coated glass slides of which three were used to deplete immunomagnetically enriched as well as not enriched LCL- and PC3 cell samples. Each slide contained three anti-CD45 coated wells and two wells that were coated without antibodies for each sample type (enriched and not enriched). One slide was exclusively used to deplete a not enriched LCL- and PC3 cell sample. The mean fluorescence intensity was measured in each well before-, in between- and after washing steps. Figure 19 presents the cell capture percentage after the first washing step on these slides.

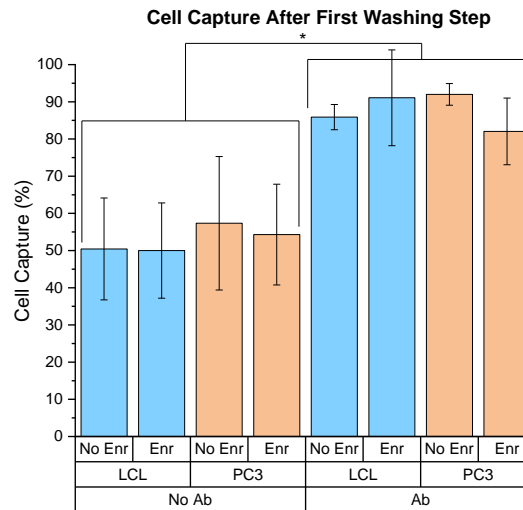


Figure 19 Cell capture percentage after the first washing step of immunomagnetically enriched and not immunomagnetically enriched (Enr and No Enr) LCL- and PC3 cell samples on an anti-CD45 coated or uncoated (Ab and No Ab) glass surface. (*Significant difference between No Ab and Ab using Welch's T-test, $p < 0.001$)

On average, 88% (S.D. 8) of cells remain on the anti-CD45 coated surface after the first washing step. The cell capture in the wells that were not coated with antibodies was 52% (S.D. 14), which is significantly lower (Welch's T-test, $p < 0.001$) than to the antibody-coated wells. This indicates that the presence of antibodies on the surface increases the cell capture. However, it does not indicate that this leads to the specific capture of LCL cells, as no significant difference was found between the LCL and PC3 cell types; overall (independent T-test, $p = 0.74$) or dependent on the coating (ANOVA, $p = 0.22$). No significant difference was observed for PC3 (ANOVA, $p = 0.21$) and LCL (ANOVA, $p = 0.37$) cell types for whether the sample was immunomagnetically enriched or not. This indicates that an additional washing step might be needed to be able wash off all unbound cells in order to deplete the sample from LCL cells and to identify if there are significant differences between the tested conditions.

Initially, it was assumed that cell capture data from independently coated slides and prepared samples could be compared. While no significant differences in cell capture between cell types were found between slides after the first washing step, this could be observed after the second washing step. However, when repeating experiments testing the same conditions on separate slides which were independently coated and using independently prepared samples, there was a variation in cell capture between experiments. An example of this can be found in Figure 20, where the mean percentage of captured cells from five separate wells (three anti-CD45 coated and two without antibodies) on a single glass slide are shown for several conditions. The images describe the results from two experiments where the same conditions were tested. The experiments were performed on different days and therefore on different slides. What stands out is the variation in cell capture between the experiments, especially in the antibody-coated wells after the second washing step.

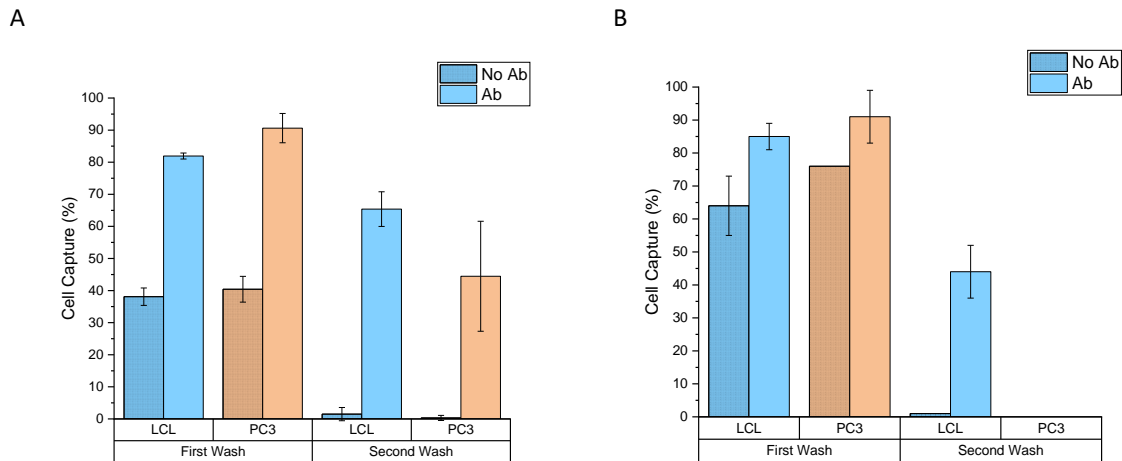


Figure 20 Cell capture percentage of live LCL and PC3 cells on an anti-CD45 antibody-coated glass (20 μ g/mL) slide in-between and after washing steps of two separate slides (A and B) prepared on separate dates, testing the same conditions.

It was postulated that the variation between experiments might be caused by a difference in the second washing step. To investigate if the second washing step's speed or duration would impact the cell capture percentage, this was tested on a single antibody-coated glass slide in wells coated with the same concentration of anti-CD45 antibodies. Table 2 describes the average capture of LCL and PC3 cells on the surface after the second washing step in separate wells. The small range of the LCL cell capture suggests that there is no significant difference in cell capture of LCL cells due to a difference in the rate of 0.5 or 2 mL/min at which washing takes place and/or duration of 5 or 20 seconds. The large range of the PC3 cell capture indicates that this might be affected by the washing speed or time but can not be concluded from this data. This was tested using a 1000 μ L micropipette tip to replicate the second washing step that is used for all multi-well slide experiments. To gather more data, this experiment was repeated (Appendix 7.2). While the same conclusions can be drawn from the second experiment, a Pasteur pipette which has a smaller opening was accidentally used instead of a 1000 μ L micropipette tip. This made it more difficult to evenly flow the washing liquid over the whole well due to the decrease in stream width, resulting in fewer cells being washed off the surface.

Table 2 The average cell capture percentage on an anti-CD45 antibody-coated glass slide using LCL and PC3 cells in a 10:1 ratio. The wells on the slide were washed at different speed and/or duration which was controlled by a syringe pump. The syringe pump was attached to a 1000 μ L micropipette tip and the average fluorescence was measured in one well per condition.

| | | Washing Speed (mL/min) | | | | |
|--------------------|----|------------------------|-----|-----|-----|-----------------------------|
| | | 0.5 | | 0.2 | | |
| | | LCL | PC3 | LCL | PC3 | |
| Washing Time (sec) | 5 | 66 | 7 | 67 | 11 | |
| | 20 | 68 | 3 | 66 | 24 | |
| | | | | | | Mean LCL 67% \pm 1 |
| | | | | | | Mean PC3 11% \pm 9 |

4.2.2 Live and Fixed Cell Samples

The cell capture percentage of LCL- and PC3 cells was investigated on an antibody-coated glass slide for a fixed cell sample which was fixed using CellSave preservative 24 hours before WBC depletion on the antibody-coated slide. The mean fluorescence intensity of six separate ROIs was measured before- and after washing steps for each condition. The calculated cell capture percentage is shown in Figure 21.

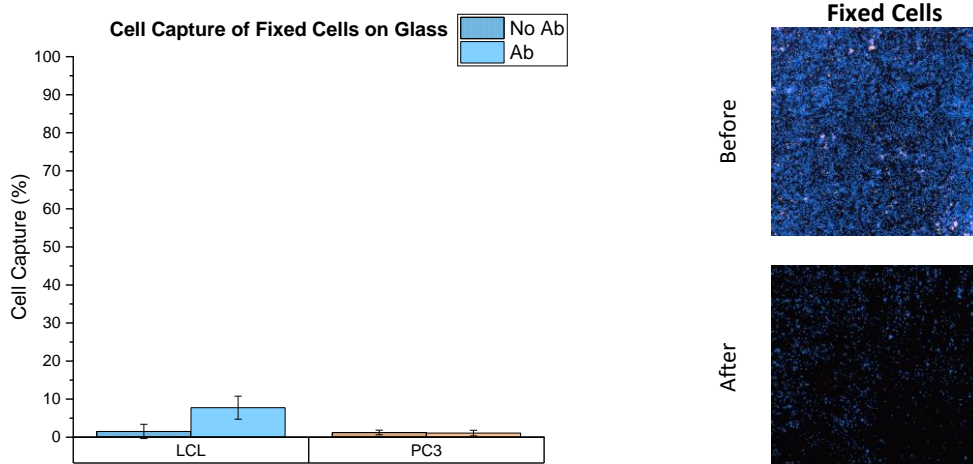


Figure 21 Cell Capture of a sample containing LCL and PC3 cells that were preserved in a CellSave preservative tube 24 hours before WBC depletion on the anti-CD45 (20 µg/mL) coated glass surface after washing steps. The images show a ROI of the slide before- and after washing.

The cell capture on the hydrogel surface of a CellSave fixed sample was tested as well, on the same slide as a live cell sample. However, this was done using an antibody concentration of 20 µg/mL, which was later found too low to capture enough cells. The average cell capture percentage was 7% of live LCL cells being captured versus 4% of fixed LCL cells making it difficult to draw conclusions.

4.2.3 Immunomagnetically Enriched Samples

To test the cell capture of immunomagnetically enriched samples on the coated surface, a comparison has been made using enriched- and not enriched samples containing live LCL and PC3 cells or fixed MNC isolated from healthy donor blood and PC3 cells. The donor blood sample was drawn 48 hours before immunomagnetic enrichment. Figure 22, Figure 23 and Figure 24 show the cell capture that was measured on a single glass- or hydrogel slide in 6 separate ROIs of 3x3mm² per condition. In the samples that were not enriched, LCL or MNC and PC3 cells were added to the well in a 10:1 ratio. To prepare the immunomagnetically enriched sample, 50 thousand PC3 cells were spiked in a sample containing 20 million LCL or MNC cells before immunomagnetic enrichment. Afterwards, the sample was distributed over five wells of which three were coated with anti-CD45 and two without antibodies.

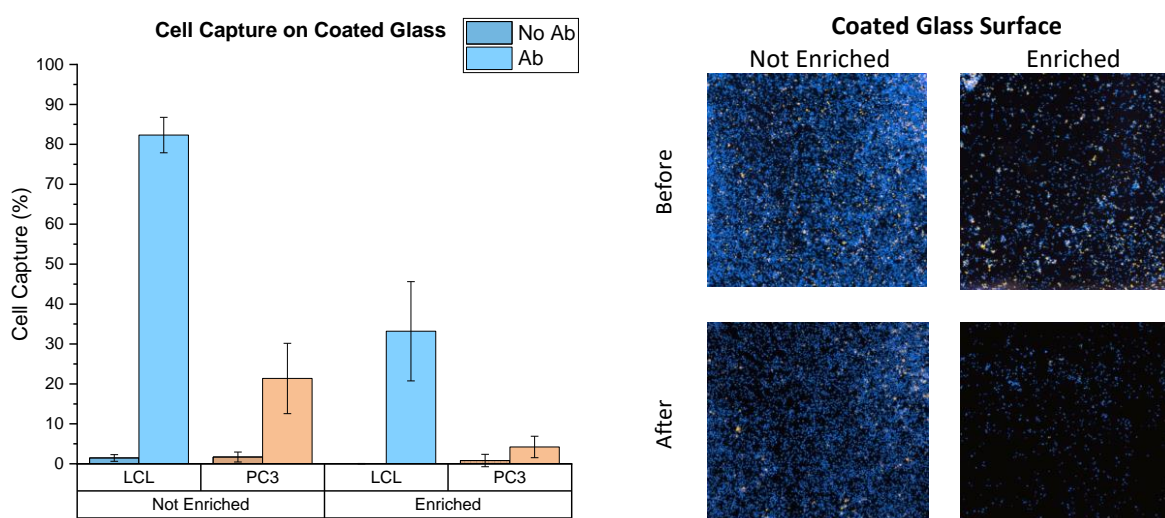


Figure 22 Cell capture percentage of a sample containing live LCL and PC3 cells and an immunomagnetically enriched sample containing live LCL and PC3 cells on an anti-CD45 antibody-coated glass surface (20 µg/mL). The mean fluorescence of six ROIs of 3x3mm² was measured for each condition. The images show a ROI of the slide before- and after washing.

In Figure 22, the measured cell capture percentage on the glass surface that was coated without antibodies is nearly zero for each condition. This indicates that nearly all cells are washed off the surface after the second washing step if no antibodies are present. On average, the percentage of captured LCL cells on the anti-CD45 coated glass surface from an enriched sample (33%) is two fifth of that of a not enriched sample (82%) (independent T-test, $p < 0.001$). For PC3 cells this is close to one-fifth (21% and 4%, respectively) (Welch's T-test, $p = 0.006$). This indicates that the cell capture of both cell types decreases when the cell sample is immunomagnetically enriched. What should be noted is that the number of cells per surface area is lower for the tested immunomagnetically enriched sample (images in Figure 22). The cell capture of LCL cells is higher than the cell capture of PC3 cells on the antibody-coated surface; fourfold in the not enriched sample (independent T-test, $p < 0.001$) and eightfold in the enriched sample (independent T-test, $p = 0.001$). Despite that, if all washed off cells are collected, the expected enrichment factor is 4.3 for a non-immunomagnetically enriched sample and 1.4 for an immunomagnetically enriched sample. While this would mean that a higher enrichment factor is reached in non-immunomagnetically enriched samples, a bigger fraction of tumor cells is 'lost' on the coated surface.

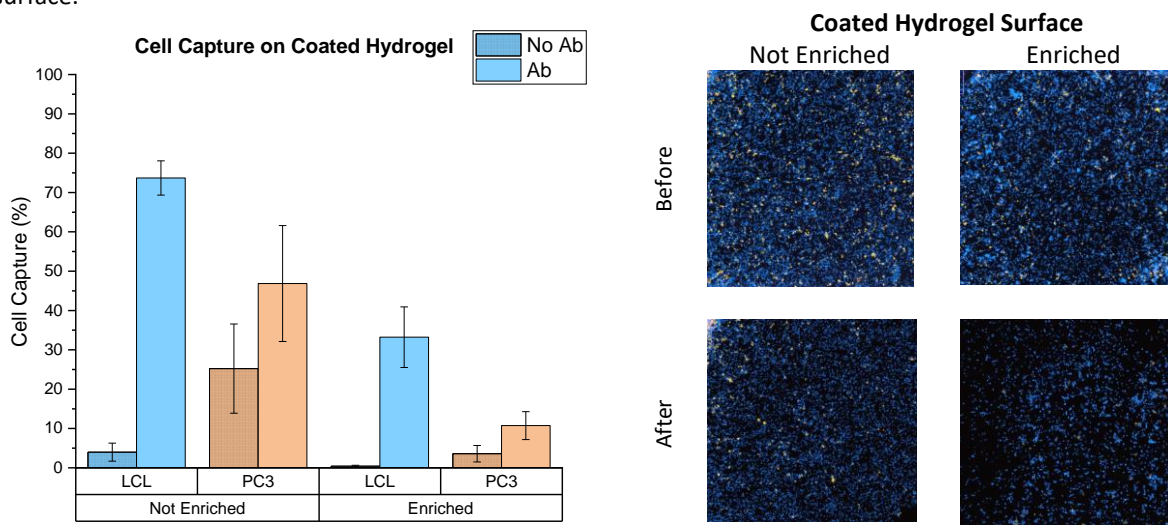


Figure 23 Cell capture percentage of a sample containing live LCL and PC3 cells and an immunomagnetically enriched sample containing live LCL and PC3 cells on an anti-CD45 antibody-coated hydrogel layer (120 µg/mL). The mean fluorescence of six ROIs of 3x3mm² was measured for each condition. The images show a ROI of the slide before- and after washing.

The measured cell capture percentage on the (antibody-)coated hydrogel layer after the second washing step can be found in Figure 23. Despite the higher PC3 cell capture, a significant difference (Welch's T-test, $p < 0.001$) in cell capture was found between the antibody-coated hydrogel surface and the hydrogel without antibodies, just as on the glass surface. However, the difference in cell capture between the two cell types is less apparent on the hydrogel: 1.6-fold in the not enriched sample (Welch's T-test, $p = 0.009$) and three-fold in the enriched sample (independent samples T-test, $p < 0.001$). No significant difference was found for the cell capture of LCL cells on the antibody-coated wells of non-immunomagnetically enriched (74%) and immunomagnetically enriched samples (33%) between both surfaces (independent samples T-test, $p = 0.844$). In comparison, the cell capture of PC3 cells (47% and 11% respectively) is higher on the hydrogel surface (Welch's T-test, $p = 0.036$): 2.2 fold for a not enriched sample and 2.8 fold when immunomagnetically enriched. Taken together, these results suggest that the non-specific binding of PC3 cells is lower on the glass surface than on the hydrogel surface while maintaining a similar cell capture percentage of LCL cells after washing steps. Besides, the expected enrichment factor on the coated hydrogel surface was 2.0 for non-immunomagnetically enriched samples and 1.3 for immunomagnetically enriched samples. While this would mean that based on this data, a higher enrichment factor is reached in non-immunomagnetically enriched samples, a larger fraction of tumor cells is 'lost' on the coated surface. However, the enrichment factor of the collected sample in live, immunomagnetically enriched samples containing LCL and PC3 cells was not measured.

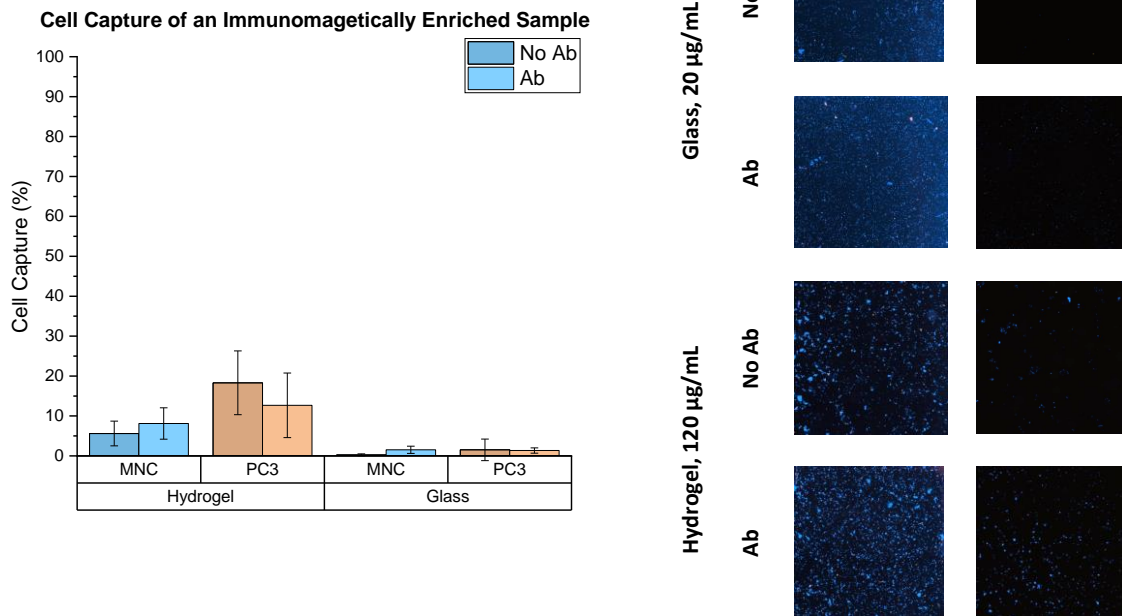


Figure 24 Cell capture percentage of an immunomagnetically enriched sample containing CellSave fixed PC3 cells and MNC isolated from healthy donor blood sample on an anti-CD45 antibody-coated surface. The mean fluorescence of six ROIs of 3x3mm² was measured for each condition. The images show a ROI of the slide before- and after washing.

To better represent a clinical sample, MNC from a healthy donor blood sample were used instead of LCL cells. After isolation of the MNCs from the whole blood sample using Ficoll, unintentionally isolated red blood cells were present in the sample. It is important not to have red blood cells in the sample that is added to the coated surface. Namely, the RBC occupy a large portion of the surface area, possibly preventing WBCs from binding to the surface or hindering tumor cells from being washed off. An image of this can be found in Appendix 7.6. Fortunately, almost no RBCs are present after immunomagnetic enrichment of the samples.

The data in Figure 24 Cell capture percentage of an immunomagnetically enriched sample containing CellSave fixed PC3 cells and MNC isolated from healthy donor blood sample on an anti-CD45 antibody-coated surface. The mean fluorescence of six ROIs of 3x3mm² was measured for each condition. What is apparent from the graph is that most cells have been washed off the surface after WBC depletion on both surface types. The non-specific binding is the highest on the hydrogel surface. Moreover, the PC3 cell capture seems higher than the MNC cell capture, which will result in more PC3 cell loss than MNC depletion. However, this difference in cell capture is not significant. Besides, the images next to the graph show that only few PC3 cells were present in the sample before WBC depletion which makes it difficult to measure reliable cell capture percentages as the background plays a more prominent role in the calculation of the cell capture percentage. In reference to the previous results of WBC depletion of immunomagnetically enriched samples, the cell capture is expected to be lower than in non-immunomagnetically enriched samples. Next to that, the cell capture of fixed cells is expected to be lower than live cells. The data does show this. The MNCs were also expected to be captured more easily than LCL cells due to their higher CD45 expression. A combination of all the abovementioned factors could have led to the results presented in Figure 24. Separate effects of these factors were not tested using MNCs.

4.3 TUMOR CELL COLLECTION AFTER WHITE BLOOD CELL DEPLETION

After WBC depletion on the coated surface, the liquid that was collected during the washing steps was analysed by flow cytometry to determine the enrichment factor and if the tumor cell purity of the sample had increased.

4.3.1 Flow Channel Setup for Controlled Washing

Although the final application of a depletion approach as this will likely benefit from the ability to allow controlled washing and collection of unbound cells through a flow channel setup, initial testing resulted in an accumulation of cells in the corners of the flow channels near the exit that made it difficult to recover a sample containing all unbound cells (see Appendix 7.3). Next to that, air bubbles in the tubing and flow channel caused cells to be pulled off of the surface. To allow realistic quantification of the captured cells, it was chosen to evaluate the washing and collection ability of the microwell slide approach in this research.

4.3.2 Efficiency of WBC Depletion

Figure 25 describes the gates used to differentiate between LCL, MNC and PC3 cells in a sample before WBC depletion using coated glass surfaces. The samples containing live LCL and PC3 cells were not immunomagnetically enriched. The cells in the sample containing MNC and PC3 cells were fixed using CellSave preservative tubes and immunomagnetically enriched. The donor blood sample was drawn 96 hours before immunomagnetic enrichment. Ten thousand events were measured in each sample via flow cytometry. In Figure 25B, two clear populations are visible that are Hoechst positive, one of which is also CTO positive (Red). There is a third population of cells visible which is mostly CTO negative.

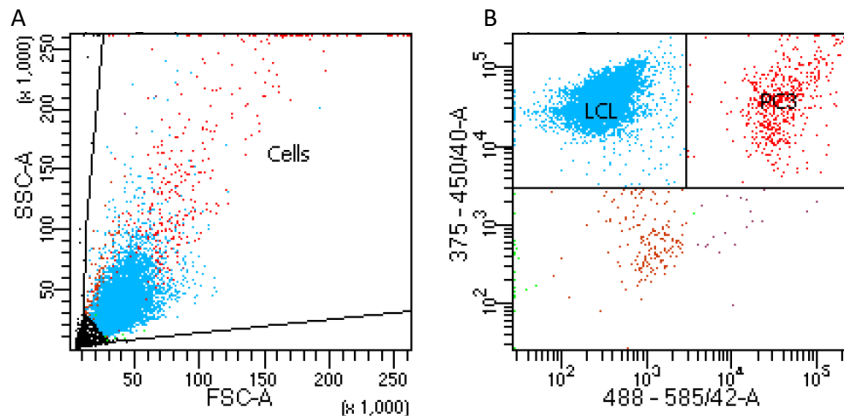


Figure 25 Scatterplots of a sample before WBC depletion containing LCL (stained with Hoechst(DAPI)) and PC3 cells (stained with Hoechst and CTO(PE)) to determine the ratio of these cell types in the sample. First, a gate was set to select cells in the sample and filter out debris (A). Then, LCL and PC3 cells were selected using gates where LCL cells were Hoechst positive and CTO negative and PC3 cells were Hoechst and CTO positive (B).

According to the plots in Figure 26, the third population is more apparent in a sample that was processed using the coated surfaces. Therefore, this population should not be neglected when assessing the efficiency of WBC depletion. As this population is mostly CTO negative and is similar to the measurement of the sample of Hoechst stained LCL cells (Appendix 7.4), it might be LCL cells. Calculations of the enrichment factor including the third population as LCL cells can be found in Appendix 7.5. However, the scatterplot in Figure 26A shows that the purple population has a low forward scatter, indicating that the measured particles are small. This could mean that the third population does not represent cells but consists of debris or dirt that is present in the washing liquid. The fact that the third population is more apparent after washing could confirm this, as the concentration of cells in this sample was lower. Therefore a higher volume of liquid was measured and thus is it more likely to measure debris.

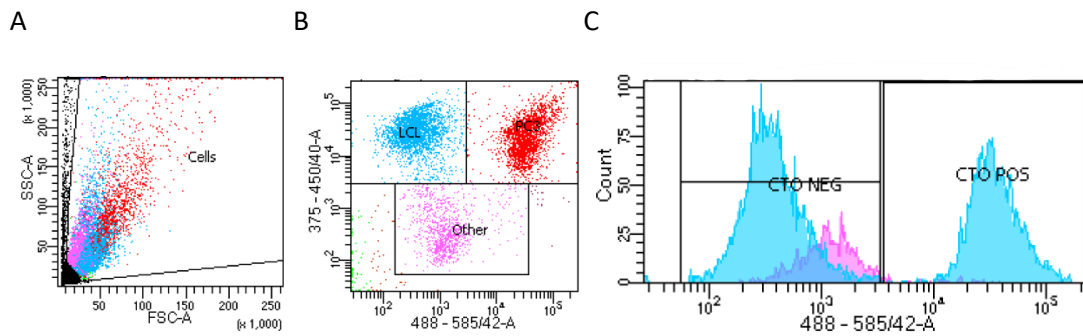


Figure 26 Scatterplot (A) presents the forward- and side scatter of the measured sample. Scatterplot (B) of a processed sample with gates distinguishing LCL (blue), PC3 (red) and an additional gate selecting a third (purple) cell population. Histogram (C) shows the two Hoechst positive populations (blue) as well as the third (purple) population. The third population is predominantly CTO negative.

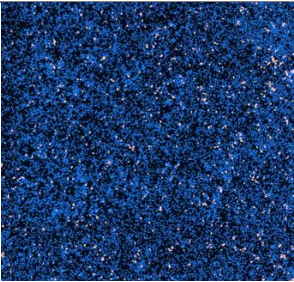
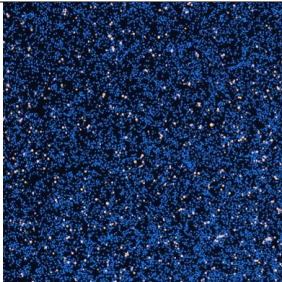

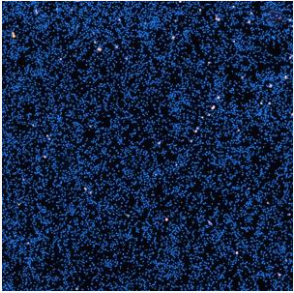
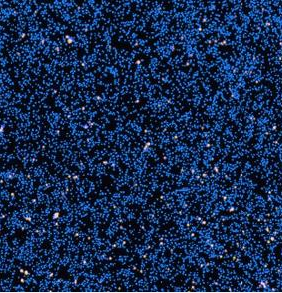

Table 3 presents the ratio of LCL- or MNC and PC3 cells that was calculated before- and after WBC depletion as well as the purity of PC3 cells in the sample and the enrichment factor in one sample per condition. Table 4 describes the expected enrichment factor which was calculated based on the cell capture percentage on the coated multiwell slide and the measured ratio of WBC and TCs in the sample before adding it to the surface. What is apparent from Table 3 is that WBC depletion on the coated multiwell slide increases in purity of TCs in the collected sample and enrichment. The enrichment factor is higher using the coated glass slide compared to the hydrogel slide. Although the ratio of the immunomagnetically enriched sample was already small before depletion by the coated glass surface, the sample was further enriched.

Table 3 Ratio of PC3 and LCL or MNC before and after WBC depletion using antibody-coated surfaces. The sample containing PC3 and MNC cells was fixed using CellSave preservative tubes and was immunomagnetically enriched before WBC depletion. The other samples contained live cells and were not immunomagnetically enriched. Calculations of the ratio, purity and enrichment factor are based on ten thousand events measured per sample.

| | BEFORE/AFTER WBC DEPLETION | PC3:LCL ON GLASS | PC3:LCL ON HYDROGEL | IMMUNOMAGNETICALLY ENRICHED PC3:MNC ON GLASS |
|----------------------|----------------------------------|------------------|---------------------|--|
| RATIO | BEFORE | 15.4 | 15.4 | 0.8 |
| | AFTER | 1.4 | 2.9 | 0.5 |
| PURITY | BEFORE | 0.1 | 0.1 | 0.6 |
| | AFTER | 0.4 | 0.3 | 0.7 |
| ENRICHMENT FACTOR | | 11.3 | 5.4 | 1.5 |

Of interest here is that the enrichment factor in the depleted sample does not agree with the expected enrichment factor based on the image analysis of the slide and is higher. This could indicate that more LCL- or MNC cells are lost during processing compared to PC3 cells. Despite that, both the expected enrichment factor and the enrichment factor calculated from the depleted sample indicate that the glass surface performs better than the hydrogel surface. This agrees with the expectation based on the results of previous experiments testing non-immunomagnetically enriched samples. Another observation is that the (fixed) immunomagnetically enriched sample containing MNC and PC3 cells already had a low concentration of cells on the surface before washing compared to the other two samples (images in Table 4).

Table 4 Images of the antibody-coated glass- and hydrogel slide before- and after washing and the expected enrichment factor based on the cell capture on the coated slide.

| | PC3:LCL ON GLASS | PC3:LCL ON HYDROGEL | IMMUNOMAGNETICALLY ENRICHED PC3:MNC ON GLASS |
|----------------------------|---|--|---|
| BEFORE WASHING |  |  |  |
| AFTER WASHING |  |  |  |
| EXPECTED ENRICHMENT FACTOR | 4.1 | 3.6 | 0.0 |

5

DISCUSSION

5.1 DISCUSSION

CTCs are rare cells that are present in the blood of metastatic cancer patients. To increase the number of CTCs that can be obtained from a patient to enable efficient characterisation of the tumor status and ultimately guide therapy, a large amount of the patient's blood needs to be screened. DLA is a method to increase the volume of blood that can be screened. However, current CTC enrichment techniques such as CellSearch encounter the problem that too much unwanted WBCs are captured along CTCs, which hinders the screening of large DLA volumes and subsequent sample analysis. A way to overcome this problem is to deplete the WBC from the previously enriched sample. As CellSearch makes use of immunomagnetic particles to enrich CTCs, it was attempted to develop and test a WBC depletion technique that can deplete immunomagnetically enriched samples. This technique makes use of antibody-coated surfaces with antiCD45-antibodies that are targeted specifically at WBCs and not CTCs.

The outcomes of this research have provided insight into the performance of the tested technology. However, the results should be interpreted with caution due to the limitations of the current research. This chapter provides a discussion of the results and a reflection on the research process and its limitations. The chapter ends with several recommendations for further research and a conclusion.

5.1.1 Antibody-coated Hydrogel- and Glass Surface

A surface was coated with anti-CD45 antibodies to specifically capture WBCs. Two surface types and corresponding coating protocols were tested; a glass- and hydrogel surface. It was expected that due to the more flexible nature of the hydrogel surface and increased antibody loading capacity, it would achieve a higher cell capture. For testing purposes, live LCL and PC3 cells were used to represent WBC and CTCs. According to the BD Quantibrite assay results, LCL cells do and PC3 cells do not express CD45 antigens and PC3 cells should therefore not bind to the anti-CD45 antibodies. These results thereby confirm the expected difference in antigen expression.

To start, an antibody concentration was selected that reached the highest antibody density on the surface and highest LCL cell capture out of the tested concentrations while keeping PC3 cell capture to a minimum; 20 $\mu\text{g}/\text{mL}$ on the glass- and 120 $\mu\text{g}/\text{mL}$ on the hydrogel surface. Even though these concentrations were selected from the ones that were tested, the shape of the trend lines in Figure 8, 9, 16, 17 and 18 indicate that the most suitable concentration might be slightly higher or lower. Despite that, the concentration that was used on the hydrogel surface was fivefold higher than on the glass surface. This confirms the hypothesis that more binding sites are present on the hydrogel surface, thereby binding more antibodies per surface area.

Contrary to expectations, the cell capture percentage of the targeted cells was not higher, but similar on both surfaces according to the results of this study. A possible explanation for this might be that the area was fully covered in cells. This is however not the case when inspecting the images of the slides before- and after washing. In fact, there is enough unoccupied area to capture even more cells on a single slide. In this project, a cell density of one-third of the calculated maximum capacity was used to prevent reaching the limit of cell occupied area. Moreover, in all experiments where the two surface types are compared (including when testing immunomagnetically enriched samples), the cell density was kept the same.

Before adding the cell sample to the wells, the sample was mixed by vortexing. However, an uneven distribution of cells in the wells was observed after centrifugation. There was a higher density of cells around the edges of the well as well as in the middle of the wells. This could have been caused by pipetting the cells in the well without additional mixing before centrifugation [56]. This way, cells gather around the outer wall of the dish due to the

pipetting pressure and the surface tension against the wall [57]. Next to that, the movement of the slide when transporting it to the centrifuge could lead to an uneven distribution.

Besides the similar LCL cell capture, it was found that the non-specific cell capture of PC3 cells is significantly higher on the hydrogel surface compared to the glass surface. This might be a result of the characteristics of the glass- and hydrogel surface that differ. If that is the case, the non-specific cell capture on the surface without antibodies should be higher than the glass surface as well, which is true according to findings of this research. Results in Figure 15 show significant differences in cell capture of both cell types. Numerous factors can contribute to the non-specific binding of cells. For example, it could be caused by physical absorption induced by electrostatic forces or hydrophobic interactions [39,58]. While the hydrogel surface was found to have a higher immobilisation capacity, PEG-coated surfaces reportedly have a lower non-specific binding of proteins on the modified surface [39,40]. The anti-fouling properties of PEG can reduce the non-specific binding of cells to the coated surface [58]. Another possible explanation is that PC3 cells are more likely to bind non-specifically than other cell types. Observations of other research group members confirm this. Moreover, the adhesion properties might have role in the nonspecific binding of PC3 cells, considering that LCL cells are non-adherent [59]. The significantly higher cell capture on the hydrogel surface without antibodies might also be caused by the possibly less effective blocking agent ethanolamine (which is used on the hydrogel coating) compared to BSA [60]. This is indicated by the lower non-specific binding of both cell types on the antibody-coated hydrogel surface with antibodies that do not target the cell type that is added to the well. Here, binding sites are already occupied by antibodies and therefore do not need to be blocked. To identify which factors play an important role in the non-specific binding and find out how this can be prevented, further testing and optimization is needed.

Based on the differences in cell capture on the coated glass- and hydrogel slides, a higher enrichment factor was expected on the sample that was processed on the coated glass surface. According to the enrichment factor that was calculated based on the measured cell capture on the slide, as well as the measured ratio of LCL and PC3 cells of the collected sample, this expectation was fulfilled.

In addition to the ability to specifically capture WBCs, the two surface coating techniques can be compared based on the preparation time and materials that are needed. The protocols used in this study prescribe that the preparation of the coated glass surface starts two days before processing the sample. The hydrogel surface is prepared on the same day as sample processing. This is short compared to the glass surface because the hydrogel layer is already present on the glass microscope slide because it is ordered from the manufacturer that way. The preparation step in which the antibody solution is incubated on the surface is only one hour according to the hydrogel preparation protocol and overnight for the glass surface preparation protocol. It is possible that overnight incubation is not necessary for preparing the glass surface or that overnight incubation is beneficial for the coating of the hydrogel, but this was not tested. Similarly, overnight incubation of the glass slide with PEG could possibly be shortened without affecting the WBC depletion efficiency. The sample throughput on both coated surfaces can easily be expanded by increasing the surface area or by stacking multiple slides on top of each other.

5.1.2 Cell Capture of Different Cell Samples

Initially, cells from cell lines were used for testing. The expression of CD45 on LCL cells is relatively similar to that of MNC isolated from a healthy donor blood sample according to the BD Quantibrite assay and is actually 25% lower. This means that if the LCL cells can be captured while expressing less of the targeted antigen, the capture of MNC from (healthy) donor blood is expected to be even higher [47]. To test if antigen expression affects cell capture, PC3 and LnCAP cells were allowed to bind to a VU1D9-coated glass surface. An unexpected result was that only 7% of PC3 cells remained on the surface after washing, while more than 80% of PC3 cells was captured in another (similar) experiment (Figure 15). It may be that the PC3 cells were at high confluency in the cell culture flask before harvesting them which in turn can lead to clumping of cells. If cells are in clumps, they form larger objects than single cells. The bigger an object, the higher the drag force the easier the object will be washed off the surface. Additionally, if the slide is at an angle, objects with a higher mass will slide down easier due to the gravitational force. This might have led to the low cell capture in this specific experiment. The effect of cell size on the flow of cells is beneficial when washing off the larger PC3 cells compared to the LCL cells. However, in contrast to the homogenous cell size of individual cell lines, the tumor cell size of patient CTCs is heterogeneous making this less effective for small CTCs.

To enable the transport of samples and to preserve cells for an extended time period, samples can be kept in CellSave preservative tubes. The performance of the WBC depletion technique affected by the CellSave preservation was tested. The cell capture on the coated slide was expected to be reduced for all cells due to the fixation. The results indicate that less than 10 % of cells are captured on the glass surface as well as the hydrogel surface, which is a significant decrease. However, it was tested on the hydrogel surface with an antibody concentration of 20µg/mL, which is low according to previous experiments. The low cell capture due to fixation of the sample could explain the low cell capture that was measured of an immunomagnetically enriched sample containing MNC isolated from healthy donor blood and PC3 cells (Figure 24 and Table 4).

5.1.3 WBC Depletion of Immunomagnetically Enriched Samples

WBC depletion of immunomagnetically enriched samples on an anti-CD45 antibody-coated multi-well slide was tested using LCL and PC3 cells and a sample containing MNC isolated from blood (WBC) and PC3 cells that were fixed in CellSave preservative tubes. Compared to a sample that was not immunomagnetically enriched, the LCL cell capture and therefore the WBC depletion decreased after immunomagnetic enrichment. This was expected, as the presence of immunomagnetic particles on the cells might lead to steric hindrance and reduce the binding affinity of cells to the coated surface. The enrichment factor is expected to be lower as well, but this was not tested for these conditions by measuring it via flow cytometry in the collected sample. The low cell capture and enrichment factor of the fixed- and immunomagnetically enriched MNC and PC3 cell sample indicates that, to get a reliable understanding of the performance of this WBC depletion technique, further testing and optimisation is needed.

5.1.4 Analysis of the Depleted Sample

The ratio of LCL or MNC and PC3 cells was calculated for the collected sample after depletion of LCL or MNC cells. This measurement was performed for ten thousand events per sample. Therefore, the total number of cells recovered after depletion is unknown. Even though the purity of PC3 cells in the sample was improved and the samples were enriched, cells could have been lost during processing. This is substantiated by the enrichment factor based on the flow cytometry measurement being higher than the expected enrichment factor based on the cell capture on the coated slide. Therefore, experiments should be performed where cell recovery is measured. According to the flow cytometry scatterplots (Figure 26) there was a third population besides WBC and TC that was not easily identified as one of these cell types. It is possible that the Hoechst staining was metabolised out of the cells during the process as cells were kept at RT for approximately six hours. This effect is less apparent in a PC3 cell sample and could be explained by the fact that the metabolism of LCL cells is faster than that of PC3 cells. LCL cells proliferate a lot faster than PC3 cells. To slow down the metabolism of cells, the samples can be kept on ice. However, the third population might consist of cells but rather debris that absorbed some of the staining, as the size of these events is relatively small according to the forward scatter. Only few cells are found when measuring ten thousand events of a sample containing fixed MNC isolated from healthy donor blood. This is due to the high amount of debris in the sample that was isolated from the blood along with the MNC.

5.1.5 Variation Between Experiments

An important limitation of this research is that most of the results presented in this thesis are of experiments performed on a single slide and have not been repeated on separate dates. This means that the reproducibility of these experiments is not clear. The statistic analysis and the conclusion drawn from it are thereby less reliable. Even though the cell capture percentages for not immunomagnetically enriched samples measured in multiple experiments seem to match according to the presented results, a variation was found between experiments after the second washing step. Altering washing speed or -duration did not fully explain the variation between experiments based on the results of Table 2. Nonetheless, this did reveal that there is a large variation in PC3 cell capture. To find the washing speed/force and time to wash off all (or as much as possible) tumor cells and retain WBC on the coated surface, a setup should be made where this can be controlled. During this research, a flow chamber setup that could be suitable for this purpose was tested. Unfortunately, this was not further investigated due to problems with bubbles in the tubing system.

Antibody coating is performed separately for each slide that is used. To rule out if there is a variation in the antibody coating between slides, the mean fluorescence intensity of the wells stained with fluorescently labelled anti-mouse IgG from different slides should be compared. Unfortunately, this data in combination with the cell capture percentage on each slide is not available for the performed experiments. The image analysis method of the coated slides before- and after washing could also cause a variation between experiments, even though the

measured mean fluorescence intensity is normalised to the background signal of that specific slide. To have a more precise estimate of the captured cells, cells should be counted individually. This was however not possible in this research as the individual cells could not be distinguished on the images that were made using a 4x objective. If a 10x objective was used, scanning would take significantly more time, resulting in the experiment taking too long to carry out within a day.

5.1.6 Comparison to Other White Blood Cell Depletion Techniques

Firstly, it is difficult to make a clear comparison of this technique and other WBC depletion techniques because they have been tested under different conditions and results have been analysed differently. Next to that, most of these other techniques have not been tested for immunomagnetically enriched samples. While immunomagnetic WBC depletion of immunomagnetically enriched samples was reported to be not effective enough [14], other techniques exist that might be applicable to WBC depletion of immunomagnetically enriched samples. An example of this is RosetteSep, an effective, density-based WBC depletion technique that can be used to deplete DLA samples [24,25]. Testing this technique on immunomagnetically enriched samples might be interesting, despite the possible change in density and steric hindrance due to the immunomagnetic particles present on the cells in the sample that could reduce the technique's performance. Numerous microfluidic techniques have been reported that might be applicable for depletion of immunomagnetically enriched samples [37]. For example, a recently published study of a size-based microfiltration WBC depletion technique using 7µm micropores reported 96% tumor cell recovery and 99% WBC depletion in whole blood samples spiked with tumor cells at a rate of 1mL/min [31]. The tumor cells used in this research had an average size of 16µm in diameter, 60% larger than average leukocytes. In comparison to our cell capture results of the antibody-coated glass surface; 82% WBC depletion and 21% tumor cell loss for not immunomagnetically enriched samples, it is a more effective technique. While the increase in cell size due to immunomagnetic enrichment might reduce the performance of the microfiltration technique, it could be applicable to WBC depletion of immunomagnetically enriched samples. Next to that, the high flow rate will enable high sample throughput but is limited to the maximum cell capture on the microfilter. The sample throughput on the coated slide depends on the coated surface area size. Taken together the features of the abovementioned technique and possible others, this indicates that the WBC depletion technique presented in this thesis is one of many possible ways to deplete WBCs from immunomagnetically enriched samples. Further research is needed to make a reliable comparison and determine if further development of the presented technique is profitable.

5.2 RECOMMENDATIONS FOR FURTHER RESEARCH

As was previously discussed, the technique presented in this research should be further optimised to enable screening of high blood volumes through the depletion of even more WBCs from immunomagnetically enriched samples. While results show that one-third of WBCs of an immunomagnetically enriched sample is captured on the coated glass surface along with 4% of the tumor cells, the recovery of cells in the collected sample was not measured. Testing this can help understand the difference in the expected and the measured enrichment factor as well as quantify the tumor cell recovery which is very important when capturing rare cells.

To better understand the performance of the presented and other existing techniques, a comparison should be made. Therefore, alternative techniques should be tested using immunomagnetically enriched samples. Next to that, testing the WBC depletion technique using a variation of tumor cell lines and/or spiking them in (healthy) donor blood (or DLA) samples can lead to a better resemblance of a clinical sample, thereby setting a better expectation of the performance when processing patient samples.

To further optimise the technique presented in this thesis, the following recommendations should be taken into consideration. Firstly, the adhesion of cells to the coating can be improved by changing the surface coating protocol. As the coated glass surface showed lower non-specific cell capture, it is suggested to start with optimisation of this protocol. However, as it is suspected that the increased non-specific binding on the hydrogel surface can be reduced by changing the blocking procedure [39,60], this should also be tested. A possible improvement of the coating protocol on glass could be changing the length of PEG molecules, as it can increase the flexibility of the polymer chains and thereby increase the antibody binding capacity [40]. To increase the antibody binding capacity of the glass surface, a variation in PEG length should be tested.

Secondly, using different antibodies or a combination of different antibodies might increase the cell capture of WBCs on the surface. Anti-CD45 antibodies were used in this project. To increase the cell capture of targeted

cells on the surface, other WBC specific antibodies could be used such as anti-CD16, which has been found to be present on a large portion of nucleated cells in immunomagnetically enriched samples [61]. Next to that, the ideal concentration of antibodies on the surface could be further investigated. Not only the antibody density on the coated surface is important, the orientation of antibodies is crucial for the receptors on the cells to bind to. Depending on the attachment of the antibody on the surface, the antibody is oriented as “end-on”, “head-on”, “side-on” or “lying-on”. To provide the best antibody-cell binding, antigen binding regions should be directed toward the cell sample after immobilisation on the surface. As the immobilisation techniques used in this research target groups that have a high prevalence throughout the antibody surface, site-directed antibody immobilisation is difficult. Evaluating and controlling the orientation will lead to better binding of cells onto the surface resulting in improved cell capture [62,63].

The flow speed used to wash off the unbound cells should be adjusted to the binding strength of cells to the surface, because at all cells will detach at a particular flow speed [46]. This brings us to the following recommendation of developing a setup in which the flow speed can be controlled. This way, the washing speed- and time can be adjusted to wash all tumor cells off the surface to reach high tumor cell recovery rates while maintaining the maximum possible WBC depletion. An attempt to achieve this has been made during this project. It was however brought to a halt due to some problems, including the accumulation of cells at the outlet of the flow channel and air bubbles present in the tubing that arose during preparation of the setup. By solving these problems, e.g. by placing a bubble trap, a comparable system can be developed and flow rate can be controlled. Moreover, the collection of the depleted sample might be improved. To assess this, cell recovery should be investigated in-between steps to identify where cells might be lost. Besides controlled flow speed, other washing techniques could be tested such as dipping the slide in a beaker filled with liquid.

Increased cell capture could also be achieved by promoting even cell distribution on the surface. Swirling of the slide before centrifugation might lead to a more homogeneous cell distribution but swirling at a high speed might result in a high cell density in the middle of the wells [57]. In addition to this, it might be beneficial to test alternative methods to promote cell attachment to the surface such as replacing the centrifugation step with incubation of the cell sample on the slide for a certain period of time, optionally on top of a moving platform (which can swirl the slide). When there is an even distribution of cells on the surface, the number of cells per surface area can be increased, thereby upscaling the sample throughput.

Lastly, further analysis of the collected sample should be performed to test cell viability and if the cells in this sample can be used for e.g. molecular characterisation after processing. The expression of tumour-specific markers on the captured cells can be tested to determine whether captured cells are suitable for subsequent molecular analyses. For example, analysis of the DNA or RNA of the captured cells by PCR.

5.3 CONCLUSION

To truly take advantage of the increased blood volume screening via DLA, the number of contaminating WBCs present in the sample before CTC characterisation needs to be reduced. This research aimed to develop a technique to deplete WBCs from immunomagnetically enriched samples using an antibody-coated surface. The data presented in this research demonstrates that one-third of WBCs can be depleted from immunomagnetically enriched samples on an antibody-coated surface, while 96% of tumor cells are washed off. As expected, the cell capture of immunomagnetically enriched samples was significantly reduced compared to non-immunomagnetically enriched samples. This is presumed to be due to the steric hindrance of the ferrofluid particles attached to the cells. Based on tests performed with both immunomagnetically enriched and non-immunomagnetically enriched samples, the cell capture on both of the tested coated surface types is fairly similar for WBC binding, while less non-specific binding of PC3 cells was measured on the glass surface. Therefore, the coated glass surface is more suitable than the coated hydrogel surface. This is substantiated by the higher enrichment factor of a non-enriched sample on glass (11x) compared to hydrogel (5x). However, the recovery of cells in the collected sample was not measured, but merely the enrichment factor determined from a part of the sample. Moreover, the collected sample was only analysed for non-immunomagnetically enriched samples. In addition, the decreased reproducibility of experiments makes reliable comparison of experiments difficult. To get a better picture of cell recovery and the effect of cell fixation and other factors, further research and optimisation of the technique is recommended. Next to that, controlling the flow speed for washing can help find the ideal balance between WBC depletion and CTC recovery to ultimately decrease the contamination of WBCs during CTC characterisation.

In conclusion, this research presents a technique for the depletion of WBCs from immunomagnetically enriched samples using an antibody-coated glass- and hydrogel surface. Out of the two tested surface types, the coated glass surface performed best because less non-specific binding of TCs was observed. Further testing is needed to assess the cell recovery in the depleted sample. Nonetheless, the presented technique shows potential to enable the screening of large blood volumes of cancer patients through WBC depletion of immunomagnetically enriched samples.

6

REFERENCES

In this chapter, references to literature that is mentioned in this report are listed.

- [1] NKR Cijfers n.d. <https://iknl.nl/nkr-cijfers> (accessed December 2, 2022).
- [2] Keller L, Pantel K. Unravelling tumour heterogeneity by single-cell profiling of circulating tumour cells. *Nat Rev Cancer* 2019;19:553–67. doi:10.1038/s41568-019-0180-2.
- [3] Coumans FAW, Ligthart ST, Uhr JW, Terstappen LWMM. Challenges in the enumeration and phenotyping of CTC. *Clin Cancer Res* 2012;18:5711–8. doi:10.1158/1078-0432.CCR-12-1585.
- [4] Miller MC, Doyle G V., Terstappen LWMM. Significance of Circulating Tumor Cells Detected by the CellSearch System in Patients with Metastatic Breast Colorectal and Prostate Cancer. *J Oncol* 2010;2010:1–8. doi:10.1155/2010/617421.
- [5] Heitzer E, Auer M, Gasch C, Pichler M, Ulz P, Hoffmann EM, Lax S, Waldispuehl-Geigl J, Mauer mann O, Lackner C, Höfler G, Eisner F, Sill H, Samonigg H, Pantel K, Riethdorf S, Bauernhofer T, ... Speicher MR. Complex tumor genomes inferred from single circulating tumor cells by array-CGH and next-generation sequencing. *Cancer Res* 2013;73:2965–75. doi:10.1158/0008-5472.CAN-12-4140.
- [6] Ferreira MM, Ramani VC, Jeffrey SS. Circulating tumor cell technologies. *Mol Oncol* 2016;10:374–94. doi:10.1016/j.molonc.2016.01.007.
- [7] Bankó P, Lee SY, Nagygyörgy V, Zrínyi M, Chae CH, Cho DH, Telekes A. Technologies for circulating tumor cell separation from whole blood. *J Hematol Oncol* 2019;12:1–20. doi:10.1186/s13045-019-0735-4.
- [8] Coumans F, Terstappen L. Detection and Characterization of Circulating Tumor Cells by the CellSearch Approach. *Methods Mol Biol* 2015;1347:263–78. doi:10.1007/978-1-4939-2990-0_18.
- [9] Fischer JC, Niederacher D, Topp SA, Honisch E, Schumacher S, Schmitz N, Föhrding LZ, Vay C, Hoffmann I, Kaspro wicz NS, Hepp PG, Mohrmann S, Nitz U, Stresemann A, Krahn T, Henze T, Griebisch E, ... Stoecklein NH. Diagnostic leukapheresis enables reliable detection of circulating tumor cells of nonmetastatic cancer patients. *Proc Natl Acad Sci U S A* 2013;110:16580–5. doi:10.1073/pnas.1313594110.
- [10] Andree KC, Mentink A, Zeune LL, Terstappen LWMM, Stoecklein NH, Neves RP, Driemel C, Lampignano R, Yang L, Neubauer H, Fehm T, Fischer JC, Rossi E, Manicone M, Basso U, Marson P, Zamarchi R, ... de Bono JS. Toward a real liquid biopsy in metastatic breast and prostate cancer: Diagnostic LeukApheresis increases CTC yields in a European prospective multicenter study (CTCTrap). *Int J Cancer* 2018;143:2584–91. doi:10.1002/ijc.31752.
- [11] Stoecklein NH, Fischer JC, Niederacher D, Terstappen LWMM. Challenges for CTC-based liquid biopsies: Low CTC frequency and diagnostic leukapheresis as a potential solution. *Expert Rev Mol Diagn* 2016;16:147–64. doi:10.1586/14737159.2016.1123095.
- [12] Fehm TN, Meier-Stiegen F, Driemel C, Jäger B, Reinhardt F, Naskou J, Franken A, Neubauer H, Neves RPL, van Dalum G, Ruckhäberle E, Niederacher D, Rox JM, Fischer JC, Stoecklein NH. Diagnostic leukapheresis for CTC analysis in breast cancer patients: CTC frequency, clinical experiences and recommendations for standardized reporting. *Cytom Part A* 2018;93:1213–9. doi:10.1002/cyto.a.23669.
- [13] Smirnov DA, Zweitzig DR, Foulk BW, Miller MC, Doyle G V., Pienta KJ, Meropol NJ, Weiner LM, Cohen SJ, Moreno JG, Connelly MC, Terstappen LWMM, O’Hara SM. Global gene expression profiling of circulating tumor cells. *Cancer Res* 2005;65:4993–7. doi:10.1158/0008-5472.CAN-04-4330.
- [14] Sieuwerts AM, Kraan J, Bolt-De Vries J, Van Der Spoel P, Mostert B, Martens JWM, Gratama JW, Sleijfer S, Foekens JA. Molecular characterization of circulating tumor cells in large quantities of contaminating leukocytes by a multiplex real-time PCR. *Breast Cancer Res Treat* 2009;118:455–68. doi:10.1007/s10549-008-0290-0.
- [15] Swennenhuis JF, Reumers J, Thys K, Aerssens J, Terstappen LWMM. Efficiency of whole genome amplification of single circulating tumor cells enriched by CellSearch and sorted by FACS. *Genome Med* 2013;5. doi:10.1186/gm510.
- [16] De Luca F, Rotunno G, Salvianti F, Galardi F, Pestrin M, Gabellini S, Simi L, Mancini I, Vannucchi AM, Pazzagli M, Di Leo A, Pinzani P. Mutational analysis of single circulating tumor cells by next generation sequencing in metastatic breast cancer. *Oncotarget* 2016;7:26107–19. doi:10.18632/oncotarget.8431.

- [17] Di Trapani M, Manaresi N, Medoro G. DEPArray™ system: An automatic image-based sorter for isolation of pure circulating tumor cells. *Cytom Part A* 2018;93:1260–6. doi:10.1002/cyto.a.23687.
- [18] Swennenhuis JF, Tibbe AGJ, Stevens M, Katika MR, Van Dalum J, Duy Tong H, Van Rijn CJM, Terstappen LWMM. Self-seeding microwell chip for the isolation and characterization of single cells. *Lab Chip* 2015;15:3039–46. doi:10.1039/c5lc00304k.
- [19] Stevens M, Oomens L, Broekmaat J, Weersink J, Abali F, Swennenhuis J, Tibbe A. VyCAP's puncher technology for single cell identification, isolation, and analysis. *Cytom Part A* 2018;93:1255–9. doi:10.1002/cyto.a.23631.
- [20] Yang Y, Rho HS, Stevens M, Tibbe AGJ, Gardeniers H, Terstappen LWMM. Microfluidic device for DNA amplification of single cancer cells isolated from whole blood by self-seeding microwells. *Lab Chip* 2015;15:4331–7. doi:10.1039/c5lc00816f.
- [21] Neumann MHD, Schneck H, Decker Y, Schömer S, Franken A, Endris V, Pfarr N, Weichert W, Niederacher D, Fehm T, Neubauer H. Isolation and characterization of circulating tumor cells using a novel workflow combining the CellSearch® system and the CellCelector™. *Biotechnol Prog* 2017;33:125–32. doi:10.1002/btpr.2294.
- [22] Swennenhuis JF, Tibbe AGJ, Levink R, Sipkema RCJ, Terstappen LWMM. Characterization of circulating tumor cells by fluorescence in situ hybridization. *Cytom Part A* 2009;75A:520–7. doi:10.1002/cyto.a.20718.
- [23] Guglielmi R, Lai Z, Raba K, van Dalum G, Wu J, Behrens B, Bhagat AAS, Knoefel WT, Neves RPL, Stoecklein NH. Technical validation of a new microfluidic device for enrichment of CTCs from large volumes of blood by using buffy coats to mimic diagnostic leukapheresis products. *Sci Rep* 2020;10:1–9. doi:10.1038/s41598-020-77227-3.
- [24] Tamminga M, Andree KC, van den Bos H, Hiltermann TJN, Mentink A, Spierings DCJ, Lansdorp P, Timens W, Schuurung E, Terstappen LWMM, Groen HJM. Leukapheresis increases circulating tumour cell yield in non-small cell lung cancer, counts related to tumour response and survival. *Br J Cancer* 2021;126:409–18. doi:10.1038/s41416-021-01634-0.
- [25] RosetteSep™ Immunodensity Cell Isolation and Cell Separation n.d. https://www.stemcell.com/products/brands/rosettesep.html?utm_source=google&utm_medium=cpc&gclid=CjwKCAiApvebBhAvEiwAe7mHSB4SMo6w6jxPWqiwxiJ0iJ3XkoS1grps1aS4Ib9ei-ibrN1iDntP2BoCOvEQAvD_BwE (accessed November 23, 2022).
- [26] Liu Z, Fusi A, Klopocki E, Schmittl A, Tinhofer I, Nonnenmacher A, Keilholz U. Negative enrichment by immunomagnetic nanobeads for unbiased characterization of circulating tumor cells from peripheral blood of cancer patients. 2011. doi:10.1186/1479-5876-9-70.
- [27] Wu Y, Deighan CJ, Miller BL, Balasubramanian P, Lustberg MB, Zborowski M, Chalmers JJ. Isolation and analysis of rare cells in the blood of cancer patients using a negative depletion methodology. *Methods* 2013;64:169–82. doi:10.1016/j.ymeth.2013.09.006.
- [28] Lara O, Tong X, Zborowski M, Farag SS, Chalmers JJ. Comparison of two immunomagnetic separation technologies to deplete T cells from human blood samples. *Biotechnol Bioeng* 2006;94:66–80. doi:10.1002/bit.20807.
- [29] Karabacak NM, Spuhler PS, Fachin F, Lim EJ, Pai V, Ozkumur E, Martel JM, Kojic N, Smith K, Chen PI, Yang J, Hwang H, Morgan B, Trautwein J, Barber TA, Stott SL, Maheswaran S, ... Toner M. Microfluidic, marker-free isolation of circulating tumor cells from blood samples. *Nat Protoc* 2014;9:694–710. doi:10.1038/nprot.2014.044.
- [30] Asgar A, Bhagat S, Hou HW, Li LD, Lim CT, Han J. DEAN FLOW FRACTIONATION (DFF) ISOLATION OF CIRCULATING TUMOR CELLS (CTCs) FROM BLOOD. n.d.
- [31] Onoshima D, Hase T, Kihara N, Kuboyama D, Tanaka H, Ozawa N, Yukawa H, Sato M, Ishikawa K, Hasegawa Y, Ishii M, Hori M, Baba Y. Leukocyte Depletion and Size-Based Enrichment of Circulating Tumor Cells Using a Pressure-Sensing Microfiltration Device. *ACS Meas Sci Au* 2023;3:113–9. doi:10.1021/acsmeasuresciau.2c00057.
- [32] Harouaka RA, Nisic M, Zheng SY. Circulating Tumor Cell Enrichment Based on Physical Properties. *J Lab Autom* 2013;18:455–68. doi:10.1177/2211068213494391.
- [33] Gupta V, Jafferji I, Garza M, Melnikova VO, Hasegawa DK, Pethig R, Davis DW. ApoStream™, a new dielectrophoretic device for antibody independent isolation and recovery of viable cancer cells from blood. *Biomicrofluidics* 2012;6. doi:10.1063/1.4731647.
- [34] Chen K, Amontree J, Varillas J, Zhang J, George TJ, Fan ZH. Incorporation of lateral microfiltration with immunoaffinity for enhancing the capture efficiency of rare cells. *Sci Rep* 2020;10:14210. doi:10.1038/s41598-020-71041-7.
- [35] Nagrath S, Sequist L V., Maheswaran S, Bell DW, Irimia D, Ulkus L, Smith MR, Kwak EL, Digumarthy S, Muzikansky A, Ryan P, Balis UJ, Tompkins RG, Haber DA, Toner M. Isolation of rare circulating tumour cells in cancer patients by microchip technology. *Nature* 2007;450:1235–9. doi:10.1038/nature06385.
- [36] Chu CH, Liu R, Ozkaya-Ahmadov T, Boya M, Swain BE, Owens JM, Burentugs E, Bilen MA, McDonald JF, Sarioglu AF. Hybrid negative enrichment of circulating tumor cells from whole blood in a 3D-printed monolithic device. *Lab Chip* 2019;19:3427–37. doi:10.1039/c9lc00575g.
- [37] Chen Y, Li P, Huang PH, Xie Y, Mai JD, Wang L, Nguyen NT, Huang TJ. Rare cell isolation and analysis in microfluidics. *Lab Chip* 2014;14:626–45. doi:10.1039/c3lc90136j.

- [38] Powell AA, Talasaz AAH, Zhang H, Coram MA, Reddy A, Deng G, Telli ML, Advani RH, Carlson RW, Mollick JA, Sheth S, Kurian AW, Ford JM, Stockdale FE, Quake SR, Pease RF, Mindrinos MN, ... Jeffrey SS. Single cell profiling of Circulating tumor cells: Transcriptional heterogeneity and diversity from breast cancer cell lines. *PLoS One* 2012;7. doi:10.1371/journal.pone.0033788.
- [39] Piehler J, Brecht A, Geckeler KE, Gauglitz G. Surface modification for direct immunoprobes. *Biosens Bioelectron* 1996;11:579–90.
- [40] Mehne J, Markovic G, Pröll F, Schweizer N, Zorn S, Schreiber F, Gauglitz G. Characterisation of morphology of self-assembled PEG monolayers: A comparison of mixed and pure coatings optimised for biosensor applications. *Anal Bioanal Chem* 2008;391:1783–91. doi:10.1007/s00216-008-2066-0.
- [41] Chen B-M, Cheng T-L, Roffler SR. Polyethylene Glycol Immunogenicity: Theoretical, Clinical, and Practical Aspects of Anti-Polyethylene Glycol Antibodies 2021. doi:10.1021/acsnano.1c05922.
- [42] Application of 3D hydrogel microarrays in molecular diagnostics: advantages and limitations 2011. doi:10.1586/ERM.11.30.
- [43] XanTec bioanalytics GmbH | Products | SPR Sensor chips | Hydrogels n.d. https://www.xantec.com/products/spr_sensorchips/hydrogels.php#/ (accessed July 27, 2023).
- [44] Features of XanTec's HC hydrogel slides n.d. www.xantec.com (accessed July 27, 2023).
- [45] XanTec bioanalytics GmbH | Products | SPR Sensor chips | 2-D coatings n.d. https://www.xantec.com/products/spr_sensorchips/2d_coatings.php (accessed August 20, 2023).
- [46] Andree KC, Mentink A, Nguyen AT, Goldsteen P, Van Dalum G, Broekmaat JJ, Van Rijn CJM, Terstappen LWMM. Tumor cell capture from blood by flowing across antibody-coated surfaces. *Lab Chip* 2019;19:1006–12. doi:10.1039/C8LC01158C.
- [47] Ohnaga T, Takei Y, Nagata T, Shimada Y. Highly efficient capture of cancer cells expressing EGFR by microfluidic methods based on antigen-antibody association. *Sci Rep* 2018;8:12005. doi:10.1038/s41598-018-30511-9.
- [48] Rheinländer A, Schraven B, Bommhardt U. CD45 in human physiology and clinical medicine. *Immunol Lett* 2018;196:22–32. doi:10.1016/j.imlet.2018.01.009.
- [49] Wen CY, Wu LL, Zhang ZL, Liu YL, Wei SZ, Hu J, Tang M, Sun EZ, Gong YP, Yu J, Pang DW. Quick-response magnetic nanospheres for rapid, efficient capture and sensitive detection of circulating tumor cells. *ACS Nano* 2014;8:941–9. doi:10.1021/nn405744f.
- [50] Li F, Xu H, Sun P, Hu Z, Aguilar ZP. Size effects of magnetic beads in circulating tumour cells magnetic capture based on streptavidin-biotin complexation. *IET Nanobiotechnology* 2019;13:6–11. doi:10.1049/iet-nbt.2018.5104.
- [51] Hoshino K, Huang YY, Lane N, Huebschman M, Uhr JW, Frenkel EP, Zhang X. Microchip-based immunomagnetic detection of circulating tumor cells. *Lab Chip* 2011;11:3449–57. doi:10.1039/c1lc20270g.
- [52] Qin J, Alt JR, Hunsley BA, Williams TL, Fernando MR. Stabilization of circulating tumor cells in blood using a collection device with a preservative reagent. *Cancer Cell Int* 2014;14:23. doi:10.1186/1475-2867-14-23.
- [53] CELLSEARCH® | CellSave Preservative Tubes n.d. <https://www.cellsearchctc.com/product-systems-overview/cellsave-preservative-tubes> (accessed August 18, 2023).
- [54] Ichikawa T, Wang D, Miyazawa K, Miyata K, Oshima M, Fukuma T. Chemical fixation creates nanoscale clusters on the cell surface by aggregating membrane proteins. *Commun Biol* 2022;5:1–9. doi:10.1038/s42003-022-03437-2.
- [55] Pereira PM, Albrecht D, Culley S, Jacobs C, Marsh M, Mercer J, Henriques R. Fix Your Membrane Receptor Imaging: Actin Cytoskeleton and CD4 Membrane Organization Disruption by Chemical Fixation. *Front Immunol* 2019;10:432958. doi:10.3389/fimmu.2019.00675.
- [56] Davidson HW, Cepeda JR, Sekhar NS, Han J, Gao L, Sosinowski T, Zhang L. High-efficiency generation of antigen-specific primary mouse cytotoxic t cells for functional testing in an autoimmune diabetes model. *J Vis Exp* 2019;2019. doi:10.3791/59985.
- [57] Fukuma Y, Inui T, Imashiro C, Kurashina Y, Takemura K. Homogenization of initial cell distribution by secondary flow of medium improves cell culture efficiency. *PLoS One* 2020;15:e0235827. doi:10.1371/journal.pone.0235827.
- [58] Yu D, Tang L, Dong Z, Loftis KA, Ding Z, Cheng J, Qin B, Yan J, Li W. Effective reduction of non-specific binding of blood cells in a microfluidic chip for isolation of rare cancer cells. *Biomater Sci* 2018;6:2871–80. doi:10.1039/c8bm00864g.
- [59] Andree KC, van Dalum G, Terstappen LWMM. Challenges in circulating tumor cell detection by the CellSearch system. *Mol Oncol* 2016;10:395–407. doi:10.1016/j.molonc.2015.12.002.
- [60] Duan ML, Huang YM, Wu SS, Li GQ, Wang SY, Chen MH, Wang C, Liu DF, Liu CW, Lai WH. Rapid and sensitive detection of Salmonella enteritidis by a pre-concentrated immunochromatographic assay in a large-volume sample system. *RSC Adv* 2017;7:55141–7. doi:10.1039/c7ra11006e.
- [61] de Wit S, Zeune LL, Hiltermann TJN, Groen HJM, van Dalum G, Terstappen LWMM. Classification of cells in CTC-enriched samples by advanced image analysis. *Cancers (Basel)* 2018;10. doi:10.3390/cancers10100377.
- [62] Welch NG, Scoble JA, Muir BW, Pigram PJ. Orientation and characterization of immobilized antibodies for improved immunoassays (Review). *Biointerphases* 2017;12:02D301. doi:10.1116/1.4978435.

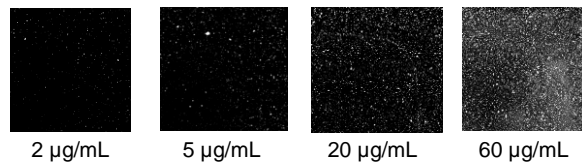
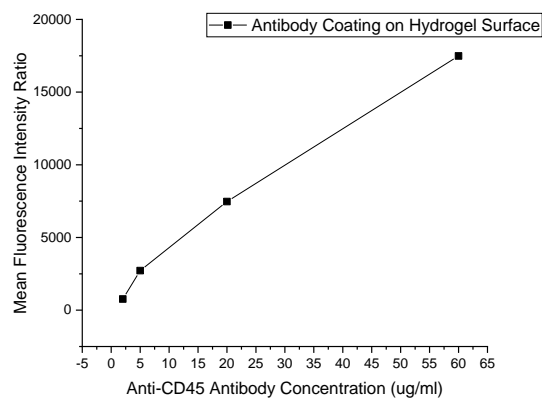
- [63] Trilling AK, Beekwilder J, Zuilhof H. Antibody orientation on biosensor surfaces: A minireview. *Analyst* 2013;138:1619–27. doi:10.1039/c2an36787d.

7

APPENDICES

7.1 ANTIBODY CONCENTRATION ON HYDROGEL

Mean Fluorescence intensity ratio of goat anti-mouse IgG-PE bound to the anti-CD45 antibody coating on a hydrogel surface after washing steps for different concentrations of anti-CD45 antibody and images of 3.5x3.5 mm² of the coated slide.



7.2 CELL CAPTURE AND WASHING SPEED AND -TIME

The average cell capture percentage on an anti-CD45 antibody-coated glass slide using LCL and PC3 cells in a 10:1 ratio. The wells on the slide were washed at different speed and/or duration which was controlled by a syringe pump. The syringe pump was attached to a 1000µL micropipette tip (B) or Pasteur pipette (A) and the average fluorescence was measured in one (B) or two (A) wells per condition.

Washing Speed (mL/min)

(A) Pasteur Pipette

| | | 0.5 | | 0.2 | | |
|---------------------------|----|---------------|---------------|---------------|---------------|--|
| | | LCL | PC3 | LCL | PC3 | |
| Washing Time (sec) | 5 | 86 (85-87) | 68 (66-71) | 79 (78-79) | 48 (47-48) | |
| | 20 | 80 (79-81) | 54 (47-62) | 81 (80-83) | 52 (44-59) | Mean LCL 82% ± 3 Mean PC3 55% ± 9 |

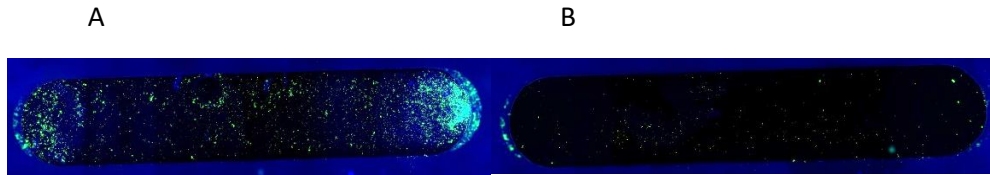
Washing Speed (mL/min)

(B) Micropipette tip (1000ul)

| | | 0.5 | | 0.2 | | |
|---------------------------|----|-----|-----|-----|-----|--|
| | | LCL | PC3 | LCL | PC3 | |
| Washing Time (sec) | 5 | 66 | 7 | 67 | 11 | |
| | 20 | 68 | 3 | 66 | 24 | Mean LCL 67% ± 1 Mean PC3 11% ± 9 |

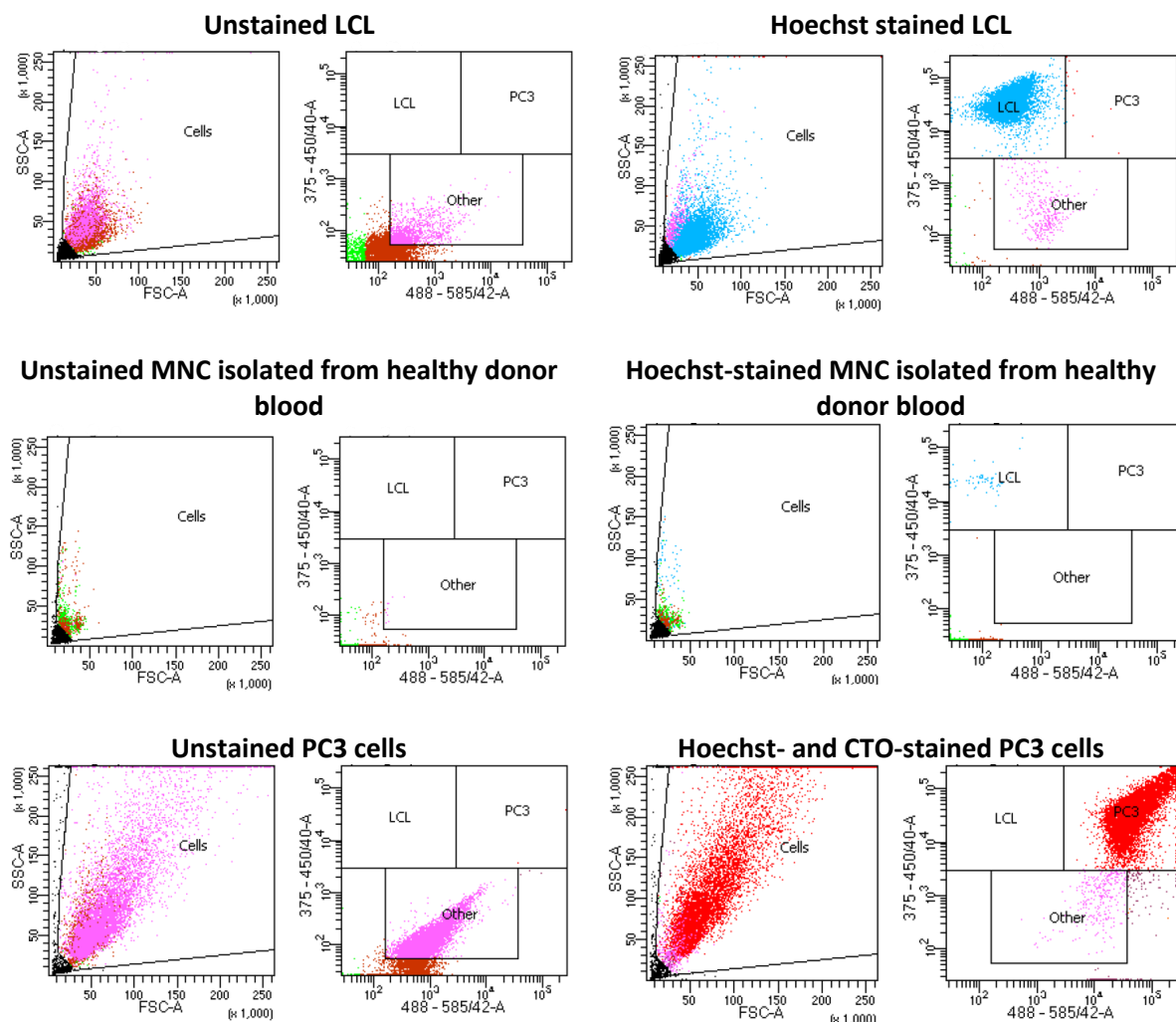
7.3 FLOW CHANNEL BEFORE- AND AFTER WASHING

Overlay images of an antibody-coated flow channel before- (A) and after (B) washing. PC3 (Cell tracker green stained, green in image) and LCL (Hoechst stained, blue in image) cells were added to the flow channel in a 1:10 ratio. Cells are accumulated at the flow channel outlet (right on image A). Most cells are washed off the surface after washing (B).



7.4 FLOW CYTOMETRY SCATTERPLOTS OF STAINED AND UNSTAINED CELLS

Flow cytometry scatterplots of unstained- and stained cells of different cell types; live LCL and PC3 cells and MNC isolated from a healthy donor blood sample that was fixed using CellSave preservative tubes. These cells were not immunomagnetically enriched.



7.5 CALCULATIONS BASED ON FLOW CYTOMETRY OF WBC DEPLETED SAMPLE INCLUDING THE THIRD POPULATION

The ratio of PC3 and LCL or MNC before and after WBC depletion using antibody-coated surfaces. The sample containing PC3 and MNC cells was fixed using CellSave preservative tubes and was immunomagnetically enriched before WBC depletion. The other samples contained live cells and were not immunomagnetically enriched. Calculations of the ratio, purity and enrichment factor are based on 10 thousand events measured per sample and are performed including or excluding the 'other' population as WBCs.

| | | IMMUNOMAGNETICALLY ENRICHED | | | | | | |
|-------------------|----------------------|-----------------------------|-------------|---------------------|------------|------------------|------------|------------|
| | | PC3:LCL ON GLASS | | PC3:LCL ON HYDROGEL | | PC3:MNC ON GLASS | | |
| | | 'Other' population as WBC | Excl. | Incl. | Excl. | Incl. | Excl. | Incl. |
| RATIO | Before WBC depletion | | 15.4 | 15.7 | 15.4 | 15.7 | 0.8 | 0.9 |
| | After WBC depletion | | 1.4 | 1.8 | 2.9 | 3.6 | 0.5 | 0.7 |
| PURITY | Before WBC depletion | | 0.1 | 0.1 | 0.1 | 0.1 | 0.6 | 0.5 |
| | After WBC depletion | | 0.4 | 0.4 | 0.3 | 0.2 | 0.7 | 0.6 |
| ENRICHMENT FACTOR | | | 11.3 | 8.7 | 5.4 | 4.4 | 1.5 | 1.3 |

7.6 RED BLOOD CELLS ON THE COATED SURFACE

Image of MNC (Blue), PC3 cells (orange) and RBC and other blood components that are present after MNC isolation using Ficoll on a coated slide before washing steps (40x objective).

